POLITECNICO DI MILANO
DIPARTIMENTO DI ELETTRONICA, INFORMAZIONE E BIOINGEGNERIA
CORSO DI LAUREA MAGISTRALE IN INGEGNERIA DELL'AUTOMAZIONE

DYNAMIC ANALYSIS AND CONTROL OF A ONCE THROUGH STEAM GENERATOR FOR A CONCENTRATED SOLAR POWER PLANT

Tesi di Laurea di:
Tommaso Maioli

Relatore:
Prof. Francesco Casella

Corelatori:
Ing. Stefano Trabucchi
Ing. Cristina Elsido

Anno Accademico 2014 - 2015

il cielo stellato sopra di me,
la legge morale dentro me

the starry sky above me
and the moral law within me

Immanuel Kant

Abstract (italiano)

FLESSIBILITÀ e continuità nella produzione di energia possono rendere gli impianti solari a concentrazione con accumulo termico competitivi nel mercato dell'energia elettrica, anche attraverso la partecipazione ai servizi di dispacciamento, finora forniti sono dagli impianti tradizionali a combustibile fossile e idroelettrici.

Il progetto PreFlexMS prevede l'introduzione nel ciclo di potenza di una caldaia a sali fusi ad attraversamento diretto, tecnologia che offre maggiori potenzialità in termini di flessibilità di esercizio rispetto ad una caldaia a corpo cilindrico, attualmente utilizzata in questo tipo di impianti.

Gli obiettivi principali del sistema di controllo sviluppato in questo lavoro sono di garantire tali requisiti e al contempo l'esercizio in condizioni di sicurezza dell'impianto.

L'analisi dinamica del ciclo di potenza ha permesso di individuare gli accoppiamenti migliori tra le variabili disponibili, punto di partenza per la definizione di una strategia di controllo di base. In primo luogo, viene proposta una logica di controllo decentralizzata basata su regolatori PI, anche se la presenza di un sistema a fase non minima ha richiesto l'utilizzo di una legge di controllo più sofisticata.
L'effettiva efficacia del sistema di controllo è stata poi verificata in un ambiente di simulazione, con un'analisi critica dei risultati. Infine, viene proposta una strategia di controllo avanzata di tipo centralizzato (MPC lineare), per esaminare quanto si può guadagnare in termini di robustezza e prestazioni quando viene richiesto di seguire riferimenti sui setpoint più rapidi.

Parole chiave: Solare a concentrazione, scambiatore ad attraversamento diretto, controllo decentralizzato, RGA, sistema a fase non minima, MPC lineare, Modelica

Abstract (english)

THE flexibility and continuity of energy production can make the concentrating solar power plants, coupled with thermal storage, more competitive in the energy market, allowing the partecipation to the dispatchability services in the same way as traditional fossil fuel and hydro power plants.

The PreFlexMS European project aims to introduce a Molten Salt Once Through Steam generator within the power unit, a technology which has greater flexibility potential if compared to steam drum boilers, currently used in those plants.

The main objective of the control system developed in this dissertation is to guarantee the aforementioned flexibility requirements, together with the security plant operation.

Through the system dynamic analysis the best couplings among the possible variables have been found, which represents the starting point of the base control strategy development. A decentralized control strategy based on PI controllers is proposed, although the presence of a non-minimum phase dynamic response has required a more sophisticated control law. The actual performance of the control system are tested into the simulation environment, with a critical analysis of the results. Finally a more advanced, centralized, control strategy is proposed (linear MPC), in order to evaluate how much the robustness and performance can be improved, when a more rapid signal tracking is requested.

Key words: CSP, OTSG, decentralized control, RGA, non-minimum phase, linear MPC, Modelica

Ringraziamenti

Prima di tutto, devo ammettere, arrivare a scrivere i ringraziamenti della mia tesi di laurea è un risultato a cui fatico ancora a credere, eppure sono qui, e scrivo.

Non è facile ripercorrere questi 5 anni e pensare a tutte le persone che mi sono state a fianco, che mi hanno fatto crescere e mi hanno dato qualcosa. Mi sforzerò, perchè credo che un po' se lo meritino e, per non dimenticare nessuno, cercherò di andare per ordine.

Il primo ringraziamento va alla mia famiglia, a mio fratello, ai miei genitori e i miei nonni. Senza il vostro aiuto probabilmente non sarei riuscito ad avere quella forza d'animo di portare a termine questo viaggio.

I miei compagni di università, Tia con cui abbiamo condiviso un sacco di belle avventure e chiaccherate, la Nic e tutti gli altri a seguire, Seba, Olga, Leonardo, Dario, Enrico, Enrico, Alessandro, Andrea, i compagni di quest'ultimo periodo passato in laboratorio (Cristina e gli MPC day!) e tutte le altre persone che ho conosciuto e con cui ho passato momenti piacevoli, cercherò di portare alta la vivacità e spensieratezza che mi avete trasmesso in tutti questi anni, che comunque mi accompagnerà per sempre.

I miei compagni di palestra (Ivana, Stefano, Andrea, Tommaso, Martina, Luca..), i miei maestri di vita, Cesare e Riccardo (e in realtà anche i miei nonni!) e tutti i ragazzi con cui ho praticato dalla Sicilia al Veneto (principalmente Jacopo, Luca, Aurora, Leonardo), passando per la Toscana, la Liguria..

Infine, ma di sicuro non per importanza, un ringraziamento speciale va a Stefano, con cui ho lavorato in questi mesi e che è sempre stata una voce

amica, quasi un fratello maggiore, sempre pronto a dare consigli e spiegarmi minuziosamente quando non capivo qualcosa e il prof. Casella per l'opportunità che mi ha dato nel partecipare in questo progetto: in questi mesi mi avete insegnato come guardare un problema e affrontarlo, studiarlo a fondo e mettere in discussione tutto per capire veramente quali sono le cause, utilizzando il pensiero critico come strumento per arrivare alla soluzione. Questo, credo, sia il più grande dono che abbiate potuto trasmettermi.

Contents

Preface **1**
Scope of work 2
PreFlexMS project description 2
Dissertation structure 4
Main findings of this study 5

1 State of the art **7**
1.1 Concentrating Solar Power (CSP) plants 7
1.1.1 Parabolic trough 8
1.1.2 Linear Fresnel 9
1.1.3 Tower plants 10
1.2 Thermal Energy storage (TES) systems 11
1.2.1 Sensible heat storage systems 12
1.3 High temperature Heat Transfer Fluids (HTF) 14
1.4 Power block 15

2 Power unit description **17**
2.1 The Rankine cycle 19
2.2 The actual implementation of the thermodynamic cycle . . . 21
2.2.1 Advantages of a Once Through Steam Generator . . . 22
2.2.2 Description of the Water Steam Cycle 23
2.3 Modes of operation of the plant 27
2.3.1 Normal continuous modes 27
2.3.2 Start-up, shut-down, and warm keeping operation modes 27

2.4 Modelling of the plant 28
2.4.1 The Modelica language 28
2.4.2 The Thermopower library 28
2.4.3 Object-oriented model of the Water-Steam Cycle . . . 29

3 System analysis and base control strategy 33
3.1 Preliminary control concepts 33
3.2 Normal operation control, purpose of the control strategy . . 34
3.2.1 Control Objectives for operation modes 34
3.2.2 Analysis of the system, main assumptions and method of analysis 35
3.2.3 Study of the linearized system 36
3.3 High load configuration 36
3.4 Low load configuration 38
3.5 Controllers tuning 40
3.5.1 Feedforward and feedback Control 41
3.5.2 Mechanical power control 42
3.5.3 Evaporation Pressure control 43
3.5.4 Feedwater temperature control 44
3.5.5 Control of the steam degree of superheating 45
3.5.6 Separator level control 51
3.6 High-low load transition 51

4 Study of Decentralized control system in realistic operational modes 55
4.1 Control Unit in the simulation environment 56
4.1.1 Additions to the control system for the implementation 56
4.2 Dispatchability 58
4.3 Warm Startup 62
4.4 Primary frequency control, preliminary study 62
4.4.1 Simulation results 64
4.4.2 Remarks on simulations results 68

5 MPC control of plant at high load 69
5.1 Linear MPC implementation 71
5.1.1 Description of Input and Outputs 71
5.1.2 Model Order Reduction 71
5.1.3 Discretization 72
5.1.4 Control Design 74
5.1.5 Selected design parameters 76
5.1.6 Setup of simulation Scenario 76
5.2 Comparison with PID decentralized control architecture . . 78

5.2.1 Discussion on the ramp-up: 78
5.2.2 Discussion on the ramp-down 81

6 Conclusions and future developments **83**

Appendices **87**

A Non-minimum Phase systems **89**
A.0.3 A closer look at non-minimum phase zeros 91

Bibliography **93**

List of Figures

1 The aim of the PreFlexMS project proposal is to 1) Adapt and 2) Integrate available technology into a product ready for market introduction. The project is structured along three axes 3

1.1 Scheme of a generic Parabolic Trough plant equipped with thermal energy storage for continuous operating. 8
1.2 The Andasol solar power station is 150-megawatt (MW) concentrated solar power station and Europe first commercial plant to use parabolic troughs. 9
1.3 Linear Fresnel system with direct steam generation. 9
1.4 The PE1 has been the first Fresnel-lens, solar power plant connected to the grid, in March 2009 10
1.5 Scheme of Solar Towers in the most common design: coupled with thermal storage to provide greater flexibility . . . 11
1.6 Gemasolar, in operation since 2011 11
1.7 working scheme of Solar Tres plant 13
1.8 Schematic diagram of a marine-type water tube boiler-see the steam drum at the top and feed drum [21] 15

2.1 Solar thermal power plant with molten salt as heat transfer and storage media. The PreflexMS-WP6 scenario 18
2.2 T-s diagram of a typical saturated Rankine cycle operating between pressures of 0.06bar and 50bar 19
2.3 T-s diagram of a typical Rankine cycle with SH and RH . . 22

2.4 Differences between conventional drum-type steam generators and OTSG 23
2.5 The High Pressure Closed feedwater heater after the Deaerator 24
2.6 diagram of the OTSG Unit, displaying the heat exchangers and the Separator 26
2.7 The complete object diagram of the Plant, displaying the preheater train, the OTSG Unit, the Turbine stages and the Control Unit 30
2.9 nonEquilibrium2phVessel 31
2.8 The model of the OTSG, displaying all the heat exchangers with relative pressure drops, sensors, and control signals . . 32

3.1 Model of the high pressure part of the plant used for linearization 35
3.2 Temperature profiles along the OTSG in two different operational points 37
3.3 MS OTSG outlet temperature as function of the recirculated mass flow through the HPH 38
3.4 Particular of the recirculation circuit 40
3.5 Bode Diagram of the transfer function between molten salt mass flow and mechanical power output 41
3.6 Open-loop transfer function Bode diagram (L(s)) and closed-loop step response (set point tracking) of the Mechanical Power at high and low load 46
3.7 Open-loop transfer function Bode diagram (L(s)) and closed-loop step response (set point tracking) of the Evaporation Pressure control at low load 47
3.8 Open-loop transfer function Bode diagram and closed-loop step response (set point tracking) of the Feedwater Temperature control at high load, controlled by θ_{BP}, and at low load, controlled by w_{SEP} 48
3.9 Step response of the open-loop transfer function between w_{FW} and ΔT_{SH} 49
3.10 90%, 70% and 60% load map of zeros and poles, where is observable the RHP zero moving towards zero, thus increasing the inverse response 50
3.11 Open loop bode plot and step response of the steam degree of superheating controller 52

4.1 Controller architecture with feedforward tables, tracking signal (that activate the controller) and switch between low and high controller (to allow a bumpless transition between the two controllers); saturations and anti-windup features are inside the PI block 57
4.2 Backward decoupler, image courtesy of IndustrialControlSystems wiki [4] 58
4.3 Dispatchability at low load: 30-40% ramp in 15 min, 900 sec. Separator is filled. 59
4.4 Dispatchability at high load: 70-80% ramp in 15 min, 900 sec. Steam degree of superheating is controlled 60
4.5 Dispatchability at transition load: 50-60% ramp in 15 min, 900 sec. Switch between low and high load control strategy 61
4.6 Startup plant, passage from 20 to 100% load ramp in less than 10 minutes (540 sec). 63
4.10 Behaviour of the power and steam degree of superheating controllers with and without backward decoupler between w_{MS} and w_{FW} 64
4.7 Preliminary primary control at low load: 30-40% ramp in 1 min. Separator is filled. 65
4.8 Preliminary primary control at high load: 70-80% ramp in 1 min. Steam degree of superheating is controlled 66
4.9 Preliminary primary control at transition load: 50-60% ramp in 1 min. Switch between low and high load control strategy 67

5.1 Diagram of the centralized linear MPC 70
5.2 I/O description of MPC 71
5.3 Bode plots of G11-G22-G33 for 100-80-60% linearized systems and 80% reduced system 73
5.4 Hankel singular values, after the 12th order the contribution to the input/output behaviour can be neglected 74
5.5 Linear MPC design parameters 76
5.6 Scenario comparison using fixed controller tuning with different linear models 77
5.7 Comparison between base control strategy and linear MPC: 60-100% ramps, 1 min each. LMPC is more robust on steam degree of superheating 79

5.8 Comparison between base control strategy and linear MPC: 100-60% ramps, 1 min each. LMPC is more robust and substantially faster in reference tracking, while acting less on manipulated variables 80

A.1 Step response of $T_n(s)$ 90
A.2 First order Padé approximation of a time-delay system . . . 92

List of Tables

3.1 RGA matrix, 100% load 38
3.2 MIMO nomenclature 38
3.3 RGA coupling at low load 39
3.4 The controller parameters for mechanical power at high and low load 43
3.5 The controller parameters for pressure at low load 44
3.6 The controller parameters for feedwater temperature control at high load (controlled by θ_{BP}) and low load (controlled by w_{SEP}) 45

Preface

Energy Context

"Let the global technology race begin!"

(I. Galiana – C. Green 2009)

Energy provision is one of the major challenges for the Human Society, and it is increasingly clear that the current production/consumption model is not sustainable on long terms, due to the wake of consequences induced by the exhaustion of fossil fuels: global climate change, local pollution, and widespread geopolitical disorders. [6]

Currently several strategy papers are defining energy developments on EU level, the most important ones being: "Energy 2020. A strategy for competitive, sustainable and secure energy" and "Energy Roadmap 2050", together with the agreements taken during COP21 summit of this year, set targets on limitations of gas emissions, increase the use of energy consumption from renewable resources and reduction in primary energy use by improving energy efficiency.

It is generally agreed that a clean energy revolution is required in order to finally decouple economic growth from the adverse environmental impact of the fossil fuel economy, and its geo-political implications. Setting emission targets can only be the starting point: in order to limit global temperature increases.

A revolution in energy technology is required, in a scenario where gov-

ernments replace emissions targets with credible long-term global commitments to invest in energy R&D, encouraging new generations to the challenge of stabilizing climate change by asking them to share their scientific and creative capabilities rather than to sacrifice future development (as it would be in the emissions-target approach). [13]

Scope of work

All power generation technologies leave their particular imprint on the power system they belong to. Wind and solar power have only recently reached significant levels of penetration in some countries, and they are expected to considerably grow even more during the next few decades, and to contribute substantially to the meeting future electricity demand, see e.g. European Commission (2011).

Wind, photovoltaic (PV) solar and concentrated solar power (CSP) with no storage have non-controllable variability, partial unpredictability and locational dependency. The downside of those plants is that they are intrinsically not dispatchable and, with large shares of these technologies predicted in the future, steps would need to be taken to ensure a continued and reliable supply of electricity. Research has been done to solve the dispatchability problem and a lot of feasible solution exists today, many of them in the field of storage systems [1].

Regarding Concentrating Solar Power (CSP) systems, big effort is put in order to permit to this technology to become truly dispatchable and penetrate actively in the energy mix to provide clean energy.
At this point, the key enabler could be the presence of Thermal Energy Storage (TES) that, in large-scale power plants (> 50 MWE) could turn the competitiveness in terms of cost and efficiency in favour of CSP plants, compared with PV plants [7] and compete with more traditional fossil fuel plants.

PreFlexMS project description

The name of the project stems from the key words “Predictability”, “Flexibility” and “Molten Salt”. In fact, this proposal aims at demonstrating and introducing into the market key enabling technologies to improve predictability and flexibility of a CSP plant with molten salt energy storage

[19].

The core objective of PreFlexMS is to enhance the predictability and flexibility of Concentrated Solar Power (CSP) generation to address the evolving needs of Regulators, Grid operators and Plant operators. Both the following technologies, yet to be demonstrated, can significantly improve the dispatchability of CSP plants:

- Molten salt steam generator based on once-through technology - Allowing fully flexible plant operation
- Integrated weather forecast and dispatch optimization - Allowing fully predictable energy dispatch.

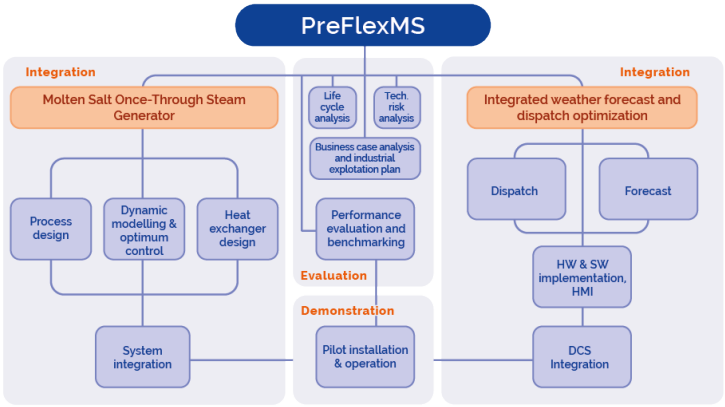

Figure 1: *The aim of the PreFlexMS project proposal is to 1) Adapt and 2) Integrate available technology into a product ready for market introduction. The project is structured along three axes*

WP6: Molten Salt Once-Through Steam Generator integration

The WorkPackage6 aims at the basic design of a full-scale molten salt once-through steam generator system (MS-OTSG) and the corresponding water and steam cycle (WSC) with optimized system integration [2].

This work package will be executed in two phases. Firstly, a full scale flexible Once-Through Steam Generator (OTSG) design will be developed for 100 MWe steam generation plants. The design shall be brought to a point in which all the key dynamic aspects of the OTSG will be clearly

outlined. Secondly, the full scale design will be scaled down to the size of the pilot. Engineering of the pilot will be carried out, bringing ahead the key design aspects in parallel, with an iterative design strategy taking into account mutual interactions between dynamics, process, control, equipment and system design. In parallel, key tests and testing strategies to validate significant aspects of the OTSG will be identified as an input for the demonstration stage. Finally, detailed engineering of equipment and system shall be carried out to provide inputs to the fabrication and procurement phases. This work package is led by: ESE (Engineering Services for Energy S.r.l.) [19].

This dissertation is devoted to the first part of the project, in which Politecnico di Milano has been a partner in the main following objectives:

- Identify the main design parameters that affect flexibility of OTSG (Once-Through Steam Generator);
- Develop process design with consideration of system dynamic behaviour and component design;
- Model the full-scale system including dynamic parameters of the OTSG;
- Develop operation and control concept, based on results of dynamic simulation;

Dissertation structure

a short description of the chapters of this thesis is given:

Chapter 1, state of the art presents the most established technologies about concentrating solar power plants, with a description of the main advantages of a solar plant with thermal storage. Ends the chapter the characterization of the Thermal Energy Storage unit (TES) taken into account in this project;

Chapter 2, power unit description describes the power unit, from the description of the thermodynamic cycle to the presentation of all the components of the Water and Steam Cycle (WSC), with the last part concerned about the modelling and the simulation environment;

Chapter 3, system analysis and base control strategy shows the analysis conducted on the system, the study of the linearized system and the description of the decentralized control strategy, whith the main objecive of control. The presence of a non-minimum phase behaviour has

required an ad-hoc controller, presented here with the methodologies used to design it;

Chapter 4, study of decentralized control system in the simulation environment deals with the tests of the control strategy presented in the simulation environment. The additions to the control architecture are presented, along with a discussion of the response of the system and the validation of the control strategy;

Chapter 5, MPC control of plant at high load is about the study of a more advanced centralized control strategy (linear MPC), which is implemented and compared with the base decentralized controller. The main target is to examine how much can be gained in terms of robustness and performance when a prompt response is requested by the system (this chapter deals with a preliminary study on primary frequency control);

Chapter 6, conclusions and future developments presents the future developments and the conclusions of this dissertation.

Main findings of this study

The contribution of this dissertation can be summerized as follows:

- dynamic analysis of the plant model, developed within the project;
- definition of a base control strategy, decentralized, based on the previous analysis conducted on the linearized system and, subsequently, the implementation of it on the non linear plant, testing the effective behaviour on different real scenarios of use (i.e. dispatchability request), to verify the validity of the proposed design.
- design of a more advanced control strategy, centralized, to verify the improvements of it compared to the base decentralized control strategy in terms of robustness and performance, when is requested a faster reference tracking on the setpoint (i.e. primary frequency control); As in the previous, the design has been studied preliminary on the linearized system and subsequently tested on the non linear system.

CHAPTER 1

State of the art

Concentrating solar plants (CSP) generate solar thermal electricity (STE) while producing no greenhouse gas emissions, so it could be a key technology for mitigating climate change. In addition, the flexibility of CSP plants enhances energy security. Unlike solar photovoltaic (PV) technologies, CSP plants use steam turbines, and thus can provide most needed ancillary services. Moreover, they can store thermal energy for later conversion to electricity [14].
If coupled with thermal energy storage (TES), CSP plants can continue to produce electricity even when solar radiation is momentary unavailable, or after sundown or in early morning when power demand steps up.
In this chapter will be introduced a description of the most used technologies among concentrating solar power plants, then will be introduced the project with a discussion on the main innovation factors.

1.1 Concentrating Solar Power (CSP) plants

Today there are three main types of concentrating technologies: Parabolic trough, concentrating linear Fresnel reflectors and solar power towers. Each of them has its own advantages and disadvantages regarding its applications

and their functioning principle. They also vary from one another in the way they focus and concentrate the sun irradiation [24].
Linear concentrator collectors capture the sun energy with large mirrors that reflect and focus the sunlight onto a linear receiver tube.
The fluid flowing in it is heated by the sunlight and then used into a Steam Generation system (producing steam directly into the collectors or through more complex systems).
Linear concentrating collector fields consist of a large number of collectors in parallel rows that are typically aligned in a north-south orientation to maximize annual and summer energy collection. With a single-axis sun-tracking system, this configuration enables the mirrors to track the sun from east to west during the day, which ensures that the sun reflects continuously onto the receiver tubes.
Central concentrator systems, in which mirrors have to track the sun position and focus the sun rays towards a point (tower systems).

1.1.1 Parabolic trough

These types of energy collectors consist on long, parabolic mirrors. Throughout the whole length of these mirrors, runs a tube that is positioned at the focal point of these parabolas. Sun irradiation is reflected by the mirror and, due to the implanted geometry, concentrated on the tube. The troughs can be aligned in a northsouth position or an east-west position and they rotate during the day to track the sunlight during daylight hours. Inside the tube, at the focal point, runs a heat transfer fluid (usually thermal oil) that absorbs the concentrated sun irradiation and rises its temperature up to 400°C [24].

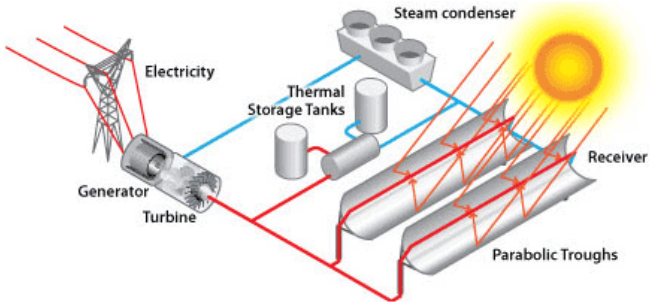

Figure 1.1: *Scheme of a generic Parabolic Trough plant equipped with thermal energy storage for continuous operating.*

The parabolic trough technology is, among all the solar thermal power sys-

tems, the one that has reached the highest level of commercial maturity. The presence of 9 SEGS plants in the Mojave Desert (USA) for a total power of 354 MWe, has pushed a strong development of the technology producing, until now, more than 13 TWh.
In Europe, this technology has been carried out recently thanks to Andasol I and II plants (100 MW), in the province of Granada, which went online in March 2009.

Figure 1.2: *The Andasol solar power station is 150-megawatt (MW) concentrated solar power station and Europe first commercial plant to use parabolic troughs.*

1.1.2 Linear Fresnel

A second linear concentrator technology is the linear Fresnel reflector system. Flat or slightly curved mirrors mounted on trackers on the ground are configured to reflect sunlight onto a receiver tube fixed in space above the mirrors. A small parabolic mirror is sometimes added atop the receiver to further focus the sunlight [24].

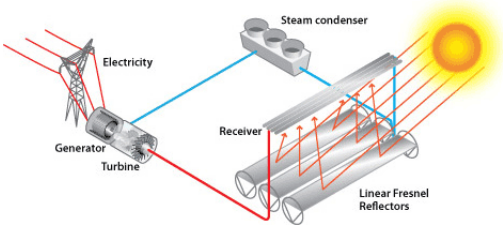

Figure 1.3: *Linear Fresnel system with direct steam generation.*

Good exploitation of land, lightness, simplicity of construction and low cost are promoting a fast development of this technology, even if low capacity of concentration and therefore low working temperatures limit its efficiency. One of the plants currently in operation (since March 2009) is the Fresnel plant 1.4 MW PE1 of Novatec Biosol, located in Murcia (South of Spain). This plant is characterized by an absorber tube placed in the focal line at 7.4 m above the ground, where water evaporates directly into saturated steam at 270°C and at a pressure of 55 bar.

Figure 1.4: *The PE1 has been the first Fresnel-lens, solar power plant connected to the grid, in March 2009*

1.1.3 Tower plants

These plants use mirrors called heliostats that track the sun by a two axes rotational movement, concentrating the sunlight onto a receiver that is normally placed at the top of a tower. In the receiver, the concentrated solar radiation is converted into thermal energy by means of a thermal fluid [24].

Early designs use these focused rays to heat water, and used the resulting steam to power a turbine. Newer designs using liquid sodium have been demonstrated, and systems using molten salts (40% potassium nitrate, 60% sodium nitrate) as the working fluids are now in operation. These working fluids have high heat capacity, which can be used as thermal storage. These designs also allow power to be generated when the plant thermal input is zero.

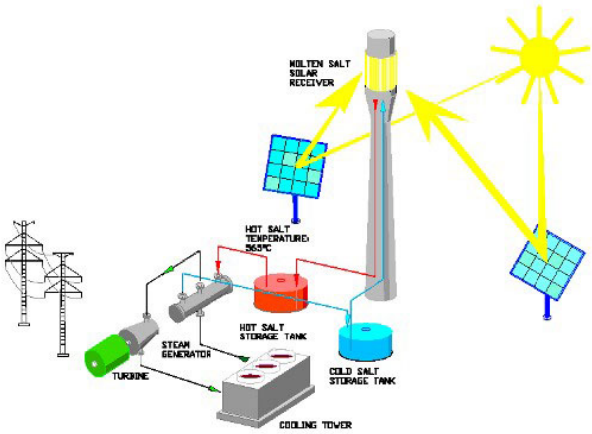

Figure 1.5: *Scheme of Solar Towers in the most common design: coupled with thermal storage to provide greater flexibility*

Gemasolar is the first commercial-scale plant in the world to apply central tower receiver and molten salt heat storage technology. The relevance of this plant lies in its technological uniqueness, since it opens up the way for new thermosolar electrical generation technology.

Figure 1.6: *Gemasolar, in operation since 2011*

1.2 Thermal Energy storage (TES) systems

The debate over the advantages and disadvantages of various solar technologies is lively [11] [12] compared PV- and CSP-based systems for large-scale solar power plants (> 50 MWE), and concluded that the cost and ef-

ficiency of storage energy can turn the competitiveness in favour of CSP systems. A potentially important benefit of CSP systems integrating TES is primarily the dispatchability;

Having the possibility to store energy thermally enables the addition of a degree of freedom in the control of the plant and gives the possibility to decide when is the right moment to produce energy, rather than be obliged to produce energy only when the sun is available.
Thus it provides grid flexibility: this feature might enable higher overall penetration of other variable generation technologies such as those based on PV cells and wind turbines [15]
The feasibility of energy storage is of paramount importance for solar power systems, to the point that it can be the technology enabler. There are many different strategies to store thermal energy in a CSP plant and the debate about which is the best option is still open, with every solution featuring his pros and cons.
There are mainly two types of TES systems, sensible storage systems and latent storage systems. As the temperature of a substance increases, its energy content also increases. The energy released (or absorbed) by a material as its temperature is reduced (or increased) is called sensible heat. On the other hand, the energy required to convert a solid material in a liquid material, or a liquid material in a vapour (phase change of a material) is called heat of fusion at the melting point (solid to liquid) and heat of vaporization (liquid to gas), respectively. Latent heat is associated with these changes of phase. [22]
As the system in this dissertation makes use of sensible heat storage, a short description of the storage working principle is described:

1.2.1 Sensible heat storage systems

Those systems consists of a storage medium, a container (commonly tank) and inlet/outlet devices. Tanks must both retain the storage material and prevent losses of thermal energy. The existence of a thermal gradient across storage is desirable but not mandatory, as it can also be overtaken using two different tank.

Active storage system

An active storage system is mainly characterized by forced convection heat transfer into the storage material. The storage medium itself circulates through a heat exchanger (this heat exchanger can also be a solar receiver

or a steam generator). This system uses one or two tanks as storage media [24].
Active systems are subdivided into direct and indirect systems. In a direct system, which is the case of the system taken into account in this work, the heat transfer fluid serves also as the storage medium, while in an indirect system, a second medium is used for storing the heat.
The system under study make use of a direct system using molten salts as HTF.

Direct system description, advantages and drawbacks

In those systems the HTF used in the solar field is also used as storage material. That means the material must reach particularly characteristics to be a good HTF and a good storage material, at the same time.
The two tanks direct system consists in a storage system where the HTF is directly stored in a hot tank, in order to be used when needed. The cooled HTF is pumped to the cold tank, where it remains waiting to be heated one more time [12].
Figure 1.8 shows the scheme of the plant Solar Tres, that uses molten salts (60% $NaNO_3$, Sodium nitrate and 40% KNO_3, Potassium nitrate) as HTF. Solar Tres is placed on Fuentes de Andalucia, near to Seville (Spain) and was built during 2008.

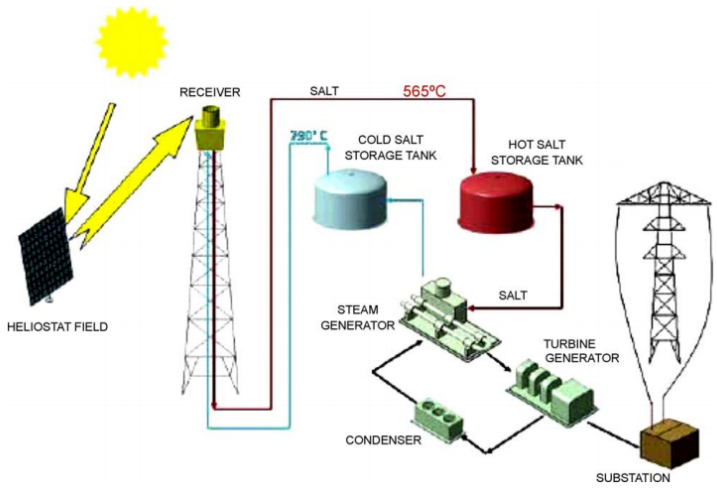

Figure 1.7: *working scheme of Solar Tres plant*

The advantages of the two tanks solar systems are:

- Low-risk approach;
- Possibility to raise the solar field output temperature to 450/500°C (in trough plants) and up to 565°C in Tower plants, thereby increasing the Rankine cycle efficiency of the power block steam turbine to the 40% range (conventional plants have a lower efficiency) [12];
- The HTF temperature rise in the collector field can increase up to a factor of 2.5 compared to Solar Two experience (located in Daggett, CA, built in 1995 and decommissioned in 1999), reducing the physical size of the thermal storage system [12] [15].

The disadvantages are:

- High cost of the heat exchangers, the need of using two tanks instead of one;
- High risk of solidification of storage fluid, due to its relatively high freeze point (which increases the M&O costs) i.e. 245 °C;

1.3 High temperature Heat Transfer Fluids (HTF)

Sensible heat storage materials are defined as a group of materials which undergo no change in phase over the temperature range encountered in the storage process. The amount of thermal energy stored in a mass of material can be expressed as:

$$E = \rho \cdot c_p \cdot V \cdot \Delta T$$

Where E is the amount of heat stored [J], ρ is the density of the storage material [$\frac{kg}{m^3}$], c_p is the average specific heat over the temperature range of operation [$\frac{J}{Kg \cdot K}$], V is the volume of storage material used (m^3), and ΔT is the temperature range of operation [°C]. The ability to store sensible thermal energy for a given material depends strongly on the value of the quantity $\rho \cdot c_p$, the thermal capacity. For a material to be useful in a TES application, it must be inexpensive and have good thermal capacity.
It is possible to store thermal energy by sensible heat in solid or liquid materials. Concerning liquid materials, a variety of fluids have been tested to transport the heat, including water, air, oil, and sodium, before molten salts were selected as best.
Molten salts are used in solar power tower systems because they are liquid at atmospheric pressure, provide an efficient, low cost medium thermal storage, their operating temperatures are compatible with today's high pressure and high-temperature steam turbines, and they are non-flammable and

non-toxic. In addition, molten salts are used in the chemical and metals industries as heat-transport fluid, so experience with molten-salt systems exists for non-solar applications [15] [22].
The Italian research laboratory ENEA has proven the technical feasibility of using molten salts in a parabolic trough solar field with salt mixtures that freeze at 220°C. Sandia National Laboratories are developing new salt mixtures with the potential for freezing points below 100°C (beyond 100°C the freezing problem is expected to be more manageable).

1.4 Power block

The state of the art of the power block part for concentrated solar power plant is the drum type boiler, which use thermal oil or molten salt as heat transfer fluid instead of fire.
The steam drum is a reservoir of water/steam at the top end of the water tubes. The drum stores the steam generated in the water tubes and acts as a phase-separator for the steam/water mixture. The difference in densities between hot and cold water helps in the accumulation of the "hotter"-water/and saturated-steam into the steam-drum [21].

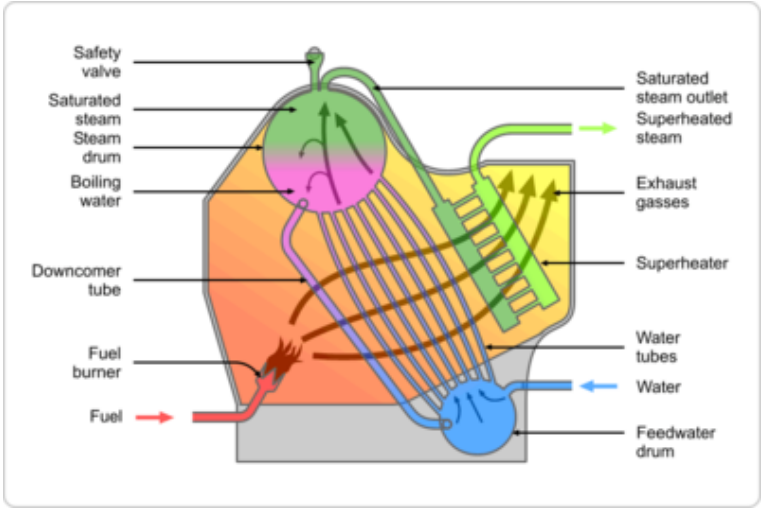

Figure 1.8: *Schematic diagram of a marine-type water tube boiler-see the steam drum at the top and feed drum [21]*

It is a well estabilished technology, used in numerous concentrated solar plants, permitting the baseload operation of the plant. The main drawback of those systems is that they are not designed for flexible operation (i.e. fast

load changes).

Once trough steam generating systems, on the other hand, have never been applied in solar but are a proven technology in the sector of gas turbine combined cycle and could permit a fully flexible combined cycle plant.

CHAPTER 2

Power unit description

This chapter contains the system description. The main system components related with the OTSG will be defined, as well as the interacting components of the cycle. In fact, the molten salt once-through steam generator is part of the water and steam cycle (WSC) and interacts with its components, as shown in the picture 2.1). The cycle efficiency is highly dependent on integration of MS-OTSG into the system.

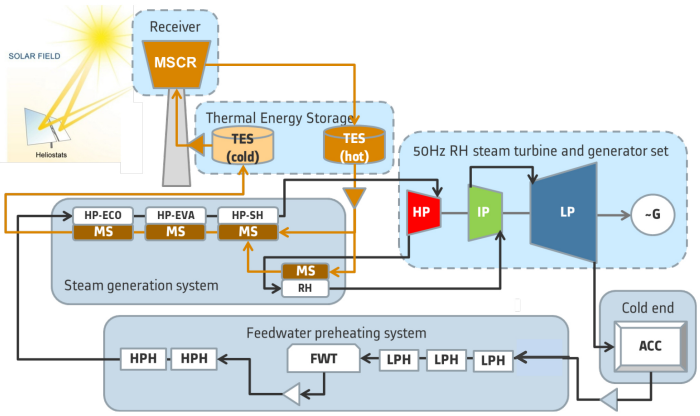

Figure 2.1: *Solar thermal power plant with molten salt as heat transfer and storage media. The PreflexMS-WP6 scenario*

The WSC is composed by:

- Feedwater preheating system, composed by a number of Low Pressure Heaters and High Pressure Heaters (LPH and HPH) with dedicated steam turbine extractions for enhanced efficiency. Such a system provides water to the OTSG at higher temperatures to prevent molten salt freezing. A deaerator in between removes undesired non-condensing gases from feedwater, in order to preserve the high temperature parts from corrosion;
- The Once Through Steam Generator unit (OTSG), composed by a molten salt preheater (HPH_{MS}), an evaporating section (ECO, EVA1, EVA2) and a superheating section (SH) in parallel with a reheating section (RH) to maximize cycle efficiency;
- Steam turbine section, composed by three main sections (high pressure, intermediate pressure and low pressure);
- Condenser section, where waste heat is rejected to the environment;
- associated piping, vessels, drains, vents, valves, desuperheating devices, and instrumentation.

Thermal energy storage (TES), composed of a hot and cold tank to store molten salts, is not part of the power unit, thus it will not be taken into account in the present analysis. The correspondent boundary condition of this system is an equivalent infinite mass source of molten salt at the constant temperature of 565°C.

2.1 The Rankine cycle

The thermodynamic cycle of the Steam Generation System is based on the simple Rankine cycle, the most common cycle for phase-changing working fluid.
The heat is supplied externally (in this case through the TES circuit) to the closed loop, which uses water as working fluid.

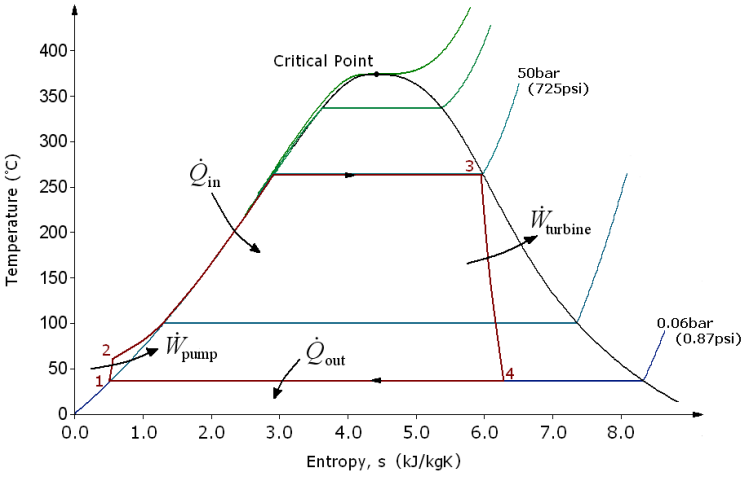

Figure 2.2: *T-s diagram of a typical saturated Rankine cycle operating between pressures of 0.06bar and 50bar*

The Rankine cycle is divided into four main processes, as follows::

- **Process 1-2:** The working fluid is pumped from low to high pressure. As the fluid is a liquid at this stage, the pump requires little input energy.
- **Process 2-3:** The high pressure liquid enters a boiler where it is heated at constant pressure by an external heat source and becomes saturated vapour. The input energy required can be easily calculated graphically, using an enthalpy-entropy chart (e.g. h-s chart or Mollier diagram), or numerically, using steam tables.
- **Process 3-4:** The saturated vapour expands through a turbine, generating power. This process decreases the temperature and pressure

of the vapour, and some condensation may occur. The output in this process can be easily calculated using the chart or tables noted above.

- **Process 4-1:** The wet vapour enters a condenser, where it is condensed at a constant pressure and becomes saturated liquid.

Variables

Q	Heat flow rate to or from the system;
w	Mass flow rate;
W	Mechanical power consumed by or provided to the system;
η_I	First principle efficiency of the process (net power output per heat input, dimensionless);
η_{pump}, η_{turb}	Isentropic efficiency of the compression (feed pump) and expansion (turbine) processes, dimensionless;
h_1, h_2, h_3, h_4	The specific enthalpies at indicated points on the T-S diagram;
h_{4s}	The turbine outlet specific enthalpy of the fluid if the turbine were isentropic;
p_1, p_2	The pressures before and after the compression process;

Equations

In general, the efficiency of a simple Rankine cycle can be written as:

$$\eta_I = \frac{W_{turb} - W_{pump}}{Q_{in}} \approx \frac{W_{turb}}{Q_{in}}$$

Each of the next four equations [25] is derived from the energy and mass balances on the working fluid control volume. η_I defines the thermodynamic efficiency of the cycle as the ratio between net power output and heat input. As the work required by the pump is often around 1% of the turbine work output, it can be simplified.

$\frac{Q_{in}}{w} = h_3 - h_2$

$\frac{Q_{out}}{w} = h_4 - h_1$

$\frac{W_{pump}}{w} = h_2 - h_1$

$\frac{W_{turb}}{w} = h_3 - h_4$

When dealing with the efficiencies of the turbines and pumps, an adjustment to the work terms must be made.

$\frac{W_{pump}}{w} = h_2 - h_1 \approx \frac{v_1 \Delta p}{\eta_{pump}} = \frac{v_1(p_2 - p_1)}{\eta_{pump}}$

$\frac{W_{turb}}{w} = h_3 - h_4 \approx (h_3 - h_2)\eta_I$

2.2 The actual implementation of the thermodynamic cycle

The actual implementation of the thermodynamic cycle differs from the simple Rankine cycle in some points:

Real Rankine cycle First, as the simple Rankine cycle presented, the actual cycle is not ideal, thus the compressions by the pumps and the expansions in the turbine are not isentropic. These processes are non-reversible and entropy thus increases. This somehow increases the power required by the pump and decreases the power generated by the turbine. In particular the efficiency of the steam turbine will be limited by water droplets formation. As the water condenses, water droplets hit the turbine blades at high speed causing pitting and erosion, gradually decreasing the life of turbine blades and efficiency of the turbine.

The easiest way to overcome this problem is superheating steam. On the T-s diagram above, state 3 is above a two phase region of wet steam so that after expansion the vapour quality would be considerably low. By superheating, state 3 will move to the right of the diagram and hence dry steam will be produced after expansion.

Rankine cycle with reheat After the dry vapour has expanded in the first turbine section, it re-enters the boiler and is reheated before passing through a second, lower-pressure, turbine section. The reheat temperature is very close or equal to the high pressure turbine inlet temperatures, whereas the optimum reheat pressure needed is only one fourth of the original boiler pressure.

Among other advantages, this prevents the vapour from condensing during its expansion and thereby damaging the turbine blades, and improves the efficiency of the cycle, because the evaporation into the cycle occurs at higher average temperature.

Regenerative Rankine cycle In the regenerative Rankine cycle, after emerging from the condenser (possibly as a subcooled liquid), the working fluid is heated by steam coming from the hot portion of the cycle. In the preheating part of the plant *steam extractions* are used to preheat the water coming from the condenser.
There is no direct contact between steam and feedwater and the heat exchange mechanism is the same of a normal shell&tube, with some modifications in design.

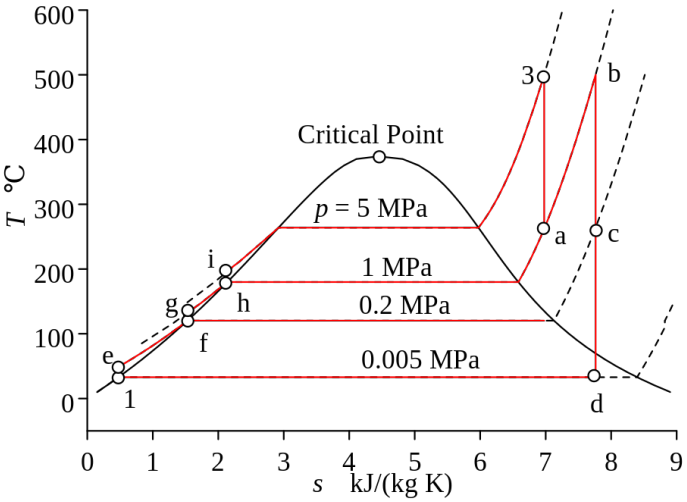

Figure 2.3: *T-s diagram of a typical Rankine cycle with SH and RH*

2.2.1 Advantages of a Once Through Steam Generator

The key feature of the plant is Flexibility, which can be achieved using a Once-Through Steam Generator, instead of a drum-type steam generator, commonly used nowadays but not conceived to have flexible operation.

Future plants, in fact, could need to be as flexible as possible and OTSG will offer better performances when compared with steam-drum heat exchangers, because of many reasons [8]:

a) successfully used in conventional and combined cycle plants, to increase flexibility:

- limitations given by steam drum thermal stresses are removed, thus allowing faster load changes, start-ups, shut-downs;
- thermal inertia of the steam generator is lower, hence allowing prompter reaction during transients and load ramps;

b) potential for cost reduction by removing costly equipment.

- steam drum itself is avoided;
- evaporator circulation pumps are smaller, compared to drum boiler;
- equipment can be assemblied in a more compact fashion;
- lowered operational costs (no power consumption of Evaporator Circulation Pumps, no blowdown heat loss).

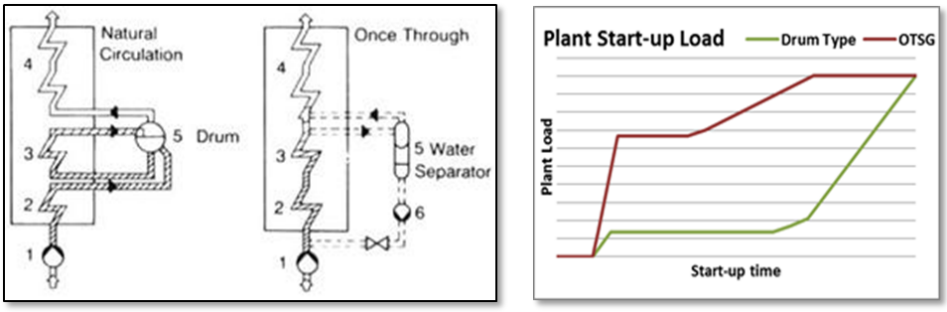

Figure 2.4: *Differences between conventional drum-type steam generators and OTSG*

2.2.2 Description of the Water Steam Cycle

The Process is designed to maximize efficiency and minimize plant cost.

The system is composed by four main parts:

- Pre-heater train;
- OTSG Unit;
- Turbine Unit;
- Condenser.

The Pre-Heater train

As discussed above, to improve cycle efficiency and prevent freezing of the molten salt in the first part of the OTSG, a train of pre-heaters has been inserted into the process.

The energy used to heat the feedwater is derived from condensing steam, extracted between the stages of the steam turbine. The percentage of the total cycle steam mass flow used for the feedwater heaters must be carefully optimized for maximum power plant thermal efficiency: in fact, increasing this fraction causes a decrease in turbine power output [27], due to lower expanding mass flow, while on the other hand the needed heat input is lower due to a higher OTSG inlet feedwater temperature (T_{FW}).

The class of preheaters used in this plants are called "closed feedwater heaters", as the steam extracted from each stage of the turbine does not mix with the feedwater going to the OTSG Unit. This solution does not require separate pumps before and after the heater to boost the feedwater to the pressure of the extracted steam, as with an open heater. The condensed steam flows to the Condenser where it finally mixes with the steam coming from the last stage of the turbine.

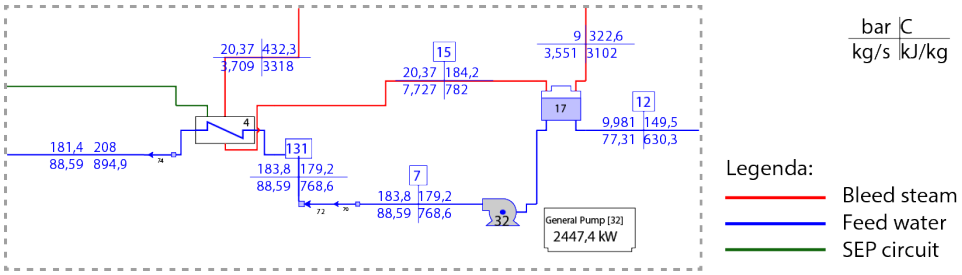

Figure 2.5: *The High Pressure Closed feedwater heater after the Deaerator*

In addition, in order to better control the feed water temperature, a bypass circuit controlled by a valve on the last heater has been added.

The Once Through Steam Generator

The OTSGs, in contrast to forced or natural circulation units, are characterized by continuous flow paths from the economizer inlet to the superheater outlet, without a steam drum in the circuit.
Specifically, the boiler used in this plant is similar to Benson design, a type of Once-Through Boiler which incorporates recirculation characteristics at

part-load operation below a certain load, as can be seen in the Fig. 2.6. However it differs from the state of the art technology of OTSG in some points:

1. the main heat exchange mechanism is convection and not radiation, as in common coal fired plants;
2. the live and RH steam temperature is almost constant at each and every load:
   - upwards it is limited by the maximum molten salt temperature;
   - downwards the Number of Thermal Units (NTU) high value of the heat exchangers push the steam temperature close to the highest molten salt temperature.

   Due to this fact, such a temperature is left uncontrolled;
3. the molten salt heat capacity is higher than air or hot gases heat capacities of a common steam generator for combined cycle application.

The boiler features 6 different shell&tube heat exchangers, in different setup:

- Hairpin for SH/RH;
- single hot pass - single cold pass, EVA2;
- double hot pass - double cold pass, ECO,EVA1;
- single hot pass - six cold pass HPH_{MS}.

HPH_{MS}: used at high loads (100-80% NCR) to increase cycle efficiency, thus a cost reduction by cooling down hot molten salt to its minimum allowed temperature.
In this way the available molten salt temperature drop exploitation is maximized while the molten salt mass flow is minimized.

ECO, EVA1 and EVA2: in the ECO the water temperature is increased till a $\Delta T_{subcooling} = 5°\text{C}$, while in EVA1 and EVA2 the phase change occurs and, at high loads (55-100% NCR), the steam produced is actually superheated. Superheating inside the evaporator depends on the available surface in the heat exchanger and it has been defined taking into account cost and feasibility of both EVA and SH. A reasonable value of $\Delta T_{superheating} = 20°\text{C}$ has been chosen.

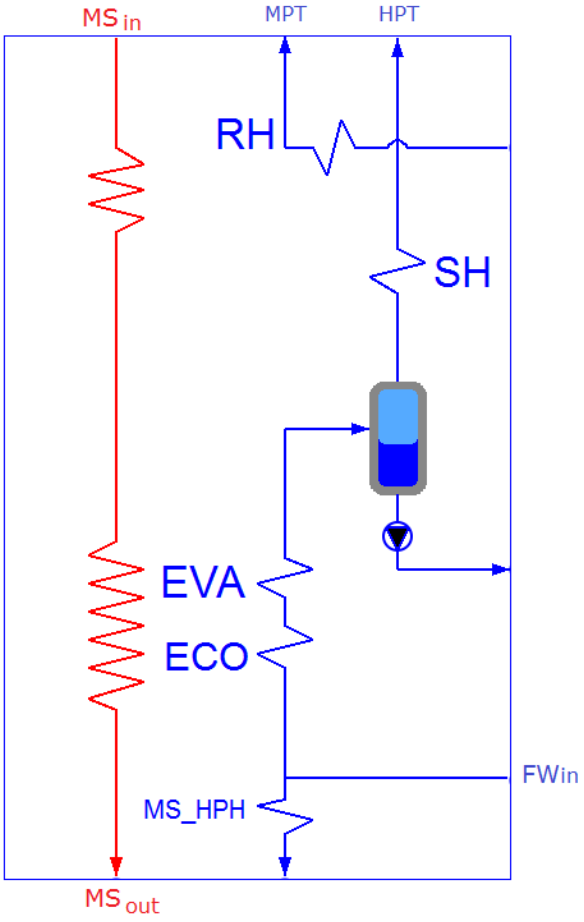

Figure 2.6: *diagram of the OTSG Unit, displaying the heat exchangers and the Separator*

SH and RH: finally, in the SH the temperature is raised till about 550 °C, close to the higher MS temperature limit, while the RH increases the temperature of the steam expanded in the first stage of the turbine till the same temperature of SH. On molten salt side, SH and RH line are connected in parallel, before mixing in the EVA section.

Separator: this component is used at low load to separate by means of gravity/cyclones, saturated steam from saturated water. The latter is recirculated to the OTSG inlet section, in order to heat up feedwater and to avoid the immission of liquid in the SH section. At high load this component is dry, thus it can be ideally seen as an inline tube.

The recirculation is guaranteed by a pump, which regulates the flow as it will be discussed in the control strategy section.

2.3 Modes of operation of the plant

The plant is designed to work in sliding pressure at high loads and constant pressure at low load.

Operation modes listed hereafter have been considered for the design and operation of the molten salt once through steam generator system and the rest of water and steam cycle.

2.3.1 Normal continuous modes

The plant must ensure the flexible operation at all admitted loads, from 100% to 20% Normal Continuous Rating (NCR). In order to achieve this goal to main modes of operation named “high load” (from 100% to 55% NCR) and “low load” operation(from 55% to 20% NCR) have been studied.

Following normal operation modes have been considered:

- NCR (Normal Continuous Rating);
- MCR (Maximum Continuous Rating) in response to primary frequency control;
- Partial load operation, in order to respect the dispatchability request.

2.3.2 Start-up, shut-down, and warm keeping operation modes

In order to permit the normal conduction of the plant, auxiliary modes of operation have been taken into account, such as:

- filling and cold start-up;
- shut-down to warm-keeping period;
- warm-keeping period, used to put the plant in “standby” during non-productive hours (e.g. during night);
- hot start-up;

Of all those modes only the hot start-up has been studied and simulated in this work.

2.4 Modelling of the plant

The design scope of the PreFlexMS-WP6 is to develope a full-scale design of a molten salt once-through steam generator system with optimized system integration into the WSC.
In this project, the Politecnico di Milano had the responsability to develop the Operation & Control Concept Design, in collaboration with ESE S.r.l., the engineering company which provided the Process Design of the plant.

The model has been developed using Modelica dynamic modeling language, through the commercial simulation environment Dymola.

2.4.1 The Modelica language

The Modelica language (The Modelica Association (2010)) is a powerful tool for the modeling of complex heterogeneous physical systems. It supports declarative equation-based modeling. This formalism enables the user to state declarative differential and algebraic equations systems(DAE), without the need to manually convert the model to ordinary differential equations systems (ODE) by solving for the derivatives, a procedure that is commonly required when using block-based modeling systems such as Simulink. Modelica is an object-oriented language which implements concepts such as classes, components (class instances), and inheritance and offers means to model, explicitly, a-causal physical interfaces which can be used to connect components together. Modelica is an open language, and it is continuously updated and maintained. Several tools are supporting the language, including Dymola, Dassault Systemes (2010), Simulation X, ITI GmbH (2010), and MapleSim, Maplesoft (2010) and the open-source modelica environment OpenModelica. Also, a freely available standard library provides basic models in different fields, including electronics, multi-body systems, and thermodynamics. [9]

2.4.2 The Thermopower library

The ThermoPower library is an open-source Modelica library for the dynamic modelling of thermal power plants and energy conversion systems. It provides basic components for system-level modelling, in particular for the study of control systems in traditional and innovative power plants and energy conversion systems.

The libray has been under continuous development at Politecnico di Milano since 2002. It has been applied to the dynamic modelling of steam

generators, combined-cycle power plants, III- and IV-generation nuclear power plants, direct steam generation solar plants, organic Rankine cycle plants, and cryogenic circuits for nuclear fusion applications. The main author is Francesco Casella, with contributions from Alberto Leva and many others. [5]

2.4.3 Object-oriented model of the Water-Steam Cycle

As it was important the study of the OTSG Unit integrated into the WSC, a model of the entire cycle has been developed, as can be seen in figure 2.7. The main model is composed of 4 parts:

- Pre-Heater train;
- Turbine Unit;
- OTSG Unit;
- Control Unit.

Since the main issue of this thesis is to assess the dynamic simulation and control of the OTSG Unit, following assumptions have been made on each part:

Pre-heater train as can be seen from the scheme, the pre-heater train is divided into two parts, the low pressure and the high pressure part, divided by the deaerator.

A **Deaerator** is a device that is widely used for the removal of oxygen and other dissolved gases from the water fed to steam-generating boilers.

From the control point of view this component works as a capacitance and to two-phase equilibrium conditions for the hydraulic circuit, since the deaerator inertia due to its volume is huge and effectively decouples the high pressure from the low pressure sections. Because our main interest is to study the High Pressure part, the Low Pressure part has been neglected in order to speed up the simulation time.

The Low Pressure train has, as inlet, the feed-water coming from the Condenser (modeled as an ideal source of mass flow) and the bleed steam extracted from the last section of the Intermediate Pressure Turbine and the two sections of the Low Pressure Turbine, used into the pre-heaters to heat up the feed-water.

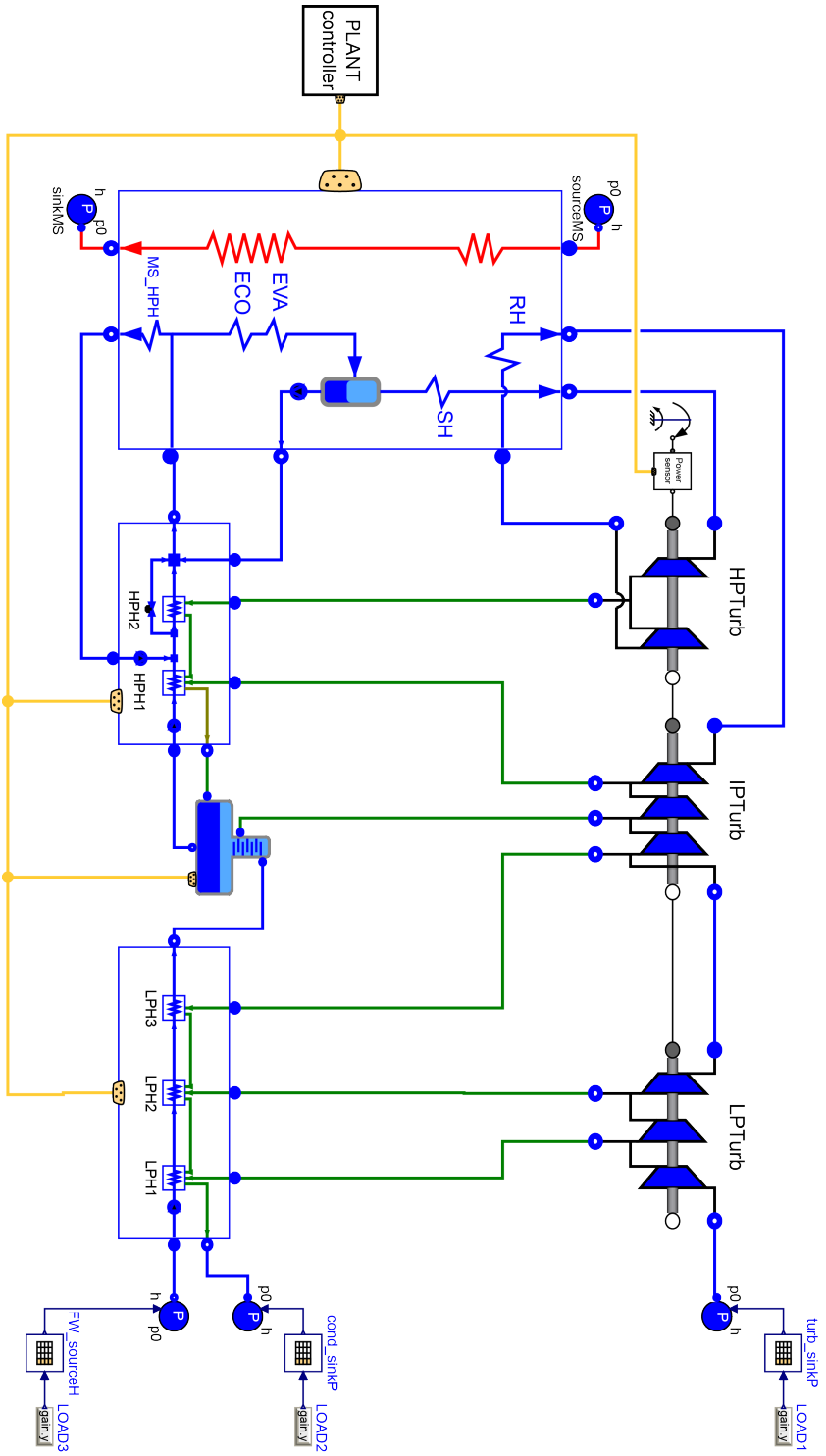

Figure 2.7: *The complete object diagram of the Plant, displaying the preheater train, the OTSG Unit, the Turbine stages and the Control Unit*

The High Pressure train has, as inlet, the feed-water coming from the Deaerator and the bleed steam extracted from the second section of the High Pressure Turbine and the first section of the Intermediate Pressure Turbine.

It also receives Saturated liquid from the Separator and from the Molten Salt high pressure heater (used partially at high load) and the bypass circuit for the second Heater.

Turbine Unit Also for the turbine sections, the main idea was to properly model the expansion of steam. Since the behaviour of each stage of the turbine can be considered as quasi-static if compared with thermal dynamics, the model of the turbine consist of two characteristic algebraic equations: the first describes the mass flow for a turbine section following Stodola Law and the second is the efficiency of the section.

OTSG Unit The model of each heat exchangers of this unit is the key-factor to correctly describe the dynamic behaviour of the cycle. Their dynamic has been described using the "$Flow1DFV$" 1D model from the Thermopower library and tuned with the heat & mass balance schemes and shell&tube design datasheet.

Inside this Unit a new component has also been developed:

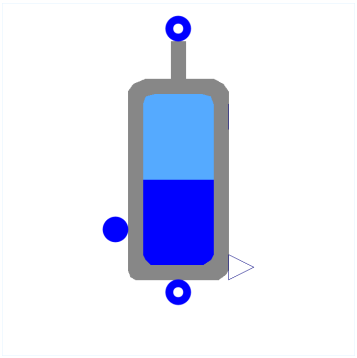

Separator. This component is actually a tank used to separate saturated steam from saturated liquid. At high loads this component is dry (because of the steam being superheated) and act as empty tube. It starts to fill between 60% and 50% NCR, when the evaporator zone of the OTSG is not able anymore to keep the temperature of feedwater at a sufficient level.

Figure 2.9: *nonEquilibrium2phVessel*

This components has as inlet the steam (or a mixture of saturated steam and saturated water) and as outlet the steam to SH, the water to OTSG inlet and the level signal to Control Unit.

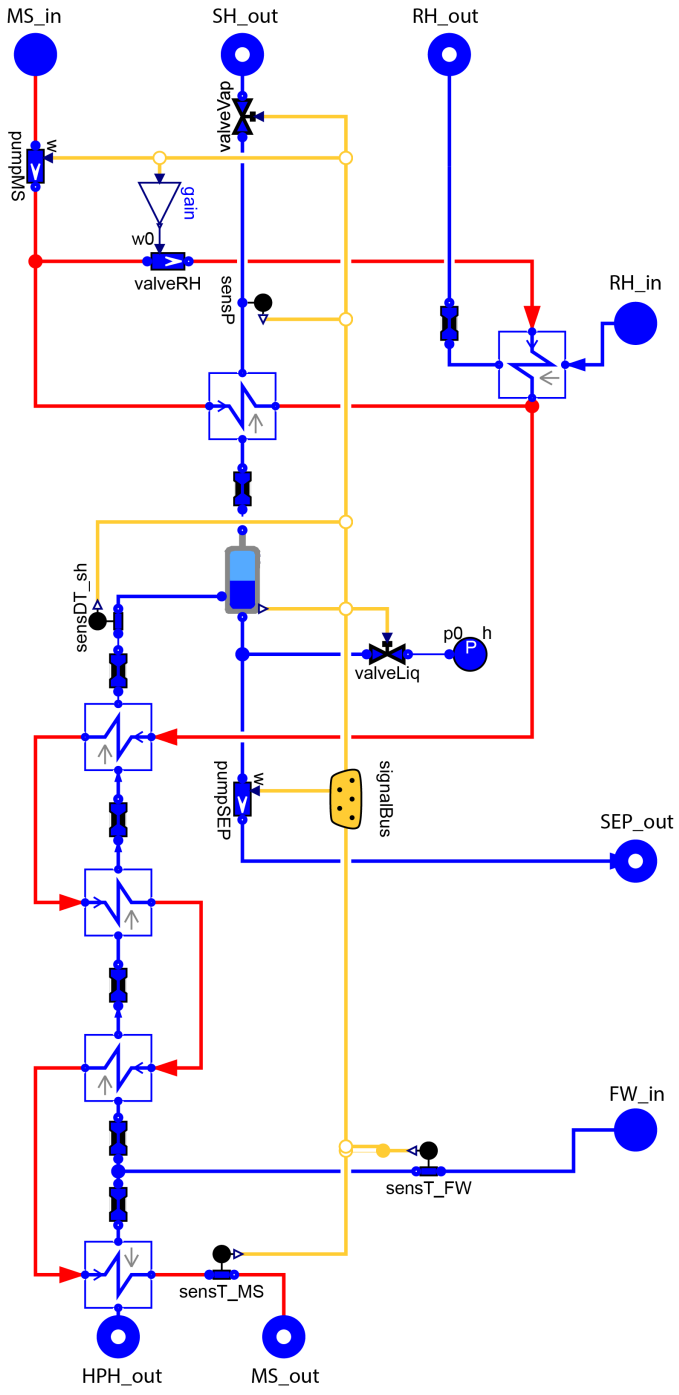

Figure 2.8: *The model of the OTSG, displaying all the heat exchangers with relative pressure drops, sensors, and control signals*

CHAPTER 3

System analysis and base control strategy

3.1 Preliminary control concepts

The aim of this chapter is to analyze and design a base control strategy for the plant, to guarantee the correct transition from a certain load to another, described by the static design.

The control strategy presented here refers to the normal operation of the plant, from 20% to 100% of the load and it is fundamental to satisfy the flexibility target presented in the introduction.
The main focus is directed to develop the simplest control strategy possible.

As a first attempt, a decentralized control strategy based mainly on PID control is proposed, though the presence of a non-minimum phase system will be the opportunity to use a more sophisticated control law. The control strategy proposed in this chapter is designed on the linearized system at different loads, and close loop performances which comply with classical control theory, are obtained. In the next chapter the strategy designed here will be tested on the non linear system, evaluating the performance of the controllers on realistic scenarios (such as dispatchability request).

3.2 Normal operation control, purpose of the control strategy

During normal operation the primary control purpose is to follow the Power reference signal and to keep all the other variables, such as temperatures and pressure, as close as possible to their nominal static values.

3.2.1 Control Objectives for operation modes

The following Control Objectives have to be fulfilled in all modes of operation:

1. power reference signal tracking;
2. molten salt freezing must be avoided;
3. minimization of thermal and mechanical stresses of plant components such as heat exchanger tubesheets;
4. pressure on water/steam side must be above pressure on molten salt side to reduce risk of molten salt contamination into water/steam cycle;
5. minimum molten salt operation temperature must be kept above 270°C;
6. maximum allowed deviation of "cold" molten salt temperature during part load at outlet of SGS (compared to 100% NCR) has to be +/- 10°C, with respect to minimum molten salt operation temperature;

As a result of the general requirements and the preliminary control strategy developed at process level, two main control strategies have been developed as function of the load demand.

The partial load process flow diagrams states that at 60% of OTSG load the feedwater temperature at OTSG inlet can be still set so that the MS outlet temperature does not go below 285°C. At 50% load the joint effects of low evaporation and extractions pressure and HPH by-pass valve saturation makes the activation of separator recirculation strictly necessary to keep the MS temperature at an acceptable value.

High load: deals with the control of the system from 55% to 100% of the load.

Low load: from 55% of the load till 20% of the load.

The "transition load" can be then set somewhere between 50% and 60% load, according to the minimum allowed value for the MS temperature. In

order to prevent the system from continually switching between the two configurations, the transition signal has to be dependent from the OTSG load and not directly from the MS temperature.

3.2.2 Analysis of the system, main assumptions and method of analysis

As discussed previously, the deaerator acts as a buffer between the high pressure and low pressure part. Taking into account the hypothesis made in the description of the model for simulation, only the high pressure part of the plant has been considered for the analysis of the plant.

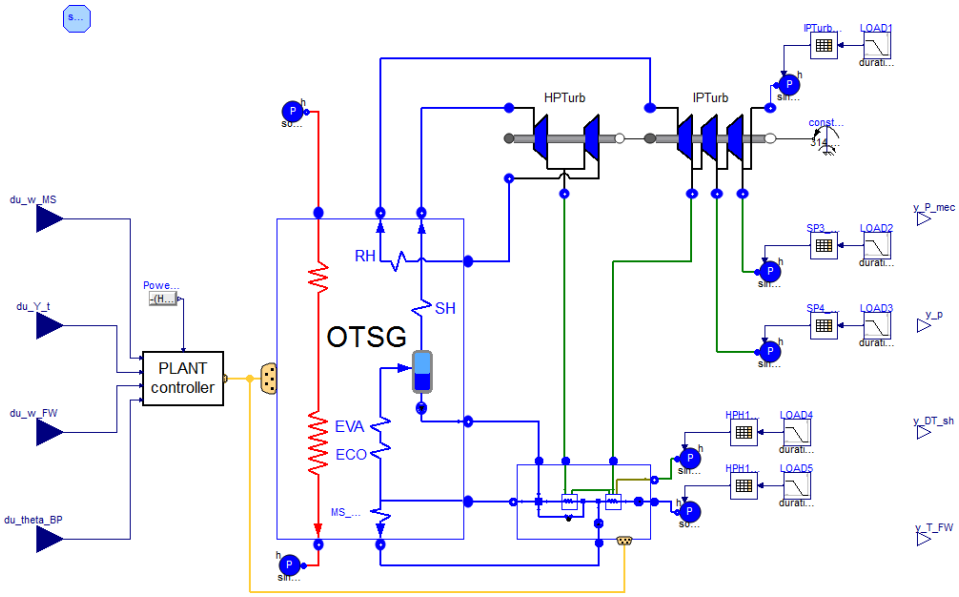

Figure 3.1: *Model of the high pressure part of the plant used for linearization*

The system has been simulated and linearized at steady state at different loads and in different configurations, using the Dymola Linearization Tool. Boundary contitions have been taken from the Heat and Mass balances as can be seen in Fig. 3.1.

Validation of the simulated system has been made by comparing the values at steady state with the values taken from the Heat and Mass balances provided by the process engineers, at different loads (from 100% NCR to 20% NCR).

Using MATLAB, different configurations have been studied and the best coupling with the minimum variables under control have been choosen,

based on the study of the RGA matrix and on the open loop dynamic response of the system.

3.2.3 Study of the linearized system

One of the main hypothesis of the classical control theory is that the system of equations describing the process has to be linear. Hence, the plant model has been linearized around equilibrium points at different loads. This procedure has been performed at different predefined loads (100%, 90%, 80%, 70%, 60%, 50%, 40%, 30%, 20%) and controllers have been tuned and validated on all the linear responses.

3.3 High load configuration

At high load operating points the available **degrees of freedom** (possible manipulated variables) are:

- hot molten salt pump mass flow rate [w_{MS}];
- turbine admittance valve, defined as $\frac{w_{TURB}}{p_{TURB}}$ [Y_t];
- feedwater general pump mass flow rate [w_{FW}];
- recirculation pump through ECO_{MS} mass flow rate [w_{ECO}];
- by-pass valve opening at HPH2 (last feedwater heater before entering Once Through) [θ_{BP}].

The desired **controlled variables** are:

- mechanical power output [P_{MEC}];
- evaporation pressure [p_{EVA}];
- feedwater OTSG inlet temperature [T_{FW}];
- MS OTSG outlet temperature [T_{MS}];
- EVA2 outlet degree of superheating (or related variable) [ΔT_{SH}].

Degree of superheating at the evaporator outlet: this variable shows a high sensitivity with regard to the feedwater mass flow. This is due to the oversized heat exchangers, which allow completely different "heat exchange configurations" against a small variation on the water/steam flow and basically constant boundary conditions, i.e. inlet/outlet OTSG temperatures of both MS and steam flows. The Fig. 3.2 shows the

temperature profiles along the OTSG for two different but close value of feedwater mass flow.

In the solid line case a higher amount of heat is exchanged in the superheating section, since the hot molten salt temperature near the vertical dashed line is lower, while for the dotted line the highest amount of heat exchanged is shifted to the evaporation section.

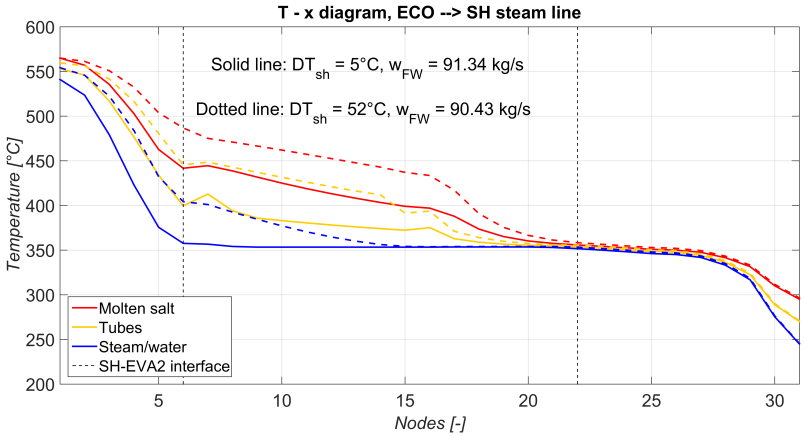

Figure 3.2: *Temperature profiles along the OTSG in two different operational points*

HPH$_{MS}$: ideally, the water mass flow recirculating through the MS high pressure heater represents a degree of freedom of the system, and could be involved in a feedback (FB) control loop. However, since its actual value is pretty low if compared with the feedwater mass flow and for load below 80-85% it is switched off, a feedforward (FF) control seems to be preferable.

This is confirmed by a simple sensitivity analysis of the system at nominal load. Through the model it is possible to evaluate the relation between the MS HPH water flow and the MS OTSG outlet temperature. As shown in Fig. 3.3 this temperature changes in a range of -2 °C/+5 °C from its nominal value, against a variation of the HPH_{MS} water mass flow of +15%/-90% from its nominal value.

Finally, the system to be controlled is a MIMO (Multi Input Multi Output) system, with four inputs and four outputs. The nomenclature of the 16 transfer functions is reported in Tab 3.2. The correct couplings between control and controlled variables is evaluated through the RGA matrix, which is reported in Tab. 3.1 for the 100% load operating point. The proposed couplings seems to be the correct ones, since the matrix is pretty

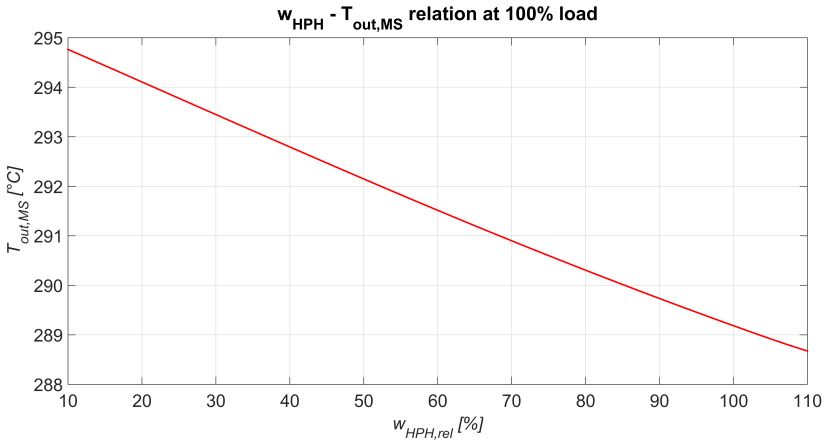

Figure 3.3: *MS OTSG outlet temperature as function of the recirculated mass flow through the HPH*

close to the identity matrix. Moreover this trend is the same for 90%, 80% 70% and 60% load, so that the control architecture has not to be changed.

		INPUT			
		Δw_{MS}	ΔY_t	Δw_{FW}	$\Delta\theta_{BP}$
OUTPUT	ΔP_{MEC}	1.17	0.16	-0.33	0.00
	Δp_{EVA}	0.17	0.85	-0.02	0.00
	$\Delta\Delta T_{SH}$	-0.39	-0.01	1.41	-0.01
	ΔT_{FW}	0.05	0.00	-0.06	1.01

Table 3.1: *RGA matrix, 100% load*

		INPUT			
		Δw_{MS}	ΔY_t	Δw_{FW}	$\Delta\theta_{BP}$
OUTPUT	ΔP_{MEC}	G_{11}	G_{12}	G_{13}	G_{14}
	Δp_{EVA}	G_{21}	G_{22}	G_{23}	G_{24}
	$\Delta\Delta T_{SH}$	G_{31}	G_{32}	G_{33}	G_{34}
	ΔT_{FW}	G_{41}	G_{42}	G_{43}	G_{44}

Table 3.2: *MIMO nomenclature*

As can be seen, the only significant coupling is between w_{MS} and w_{FW} in the power control and steam degree of superheating. Because of that, in the next chapter, dedicated to the simulation of the control system on the non linear system, a static decoupler is designed and the related improvements are presented.

3.4 Low load configuration

At low load operating points the available **degrees of freedom** are:

- hot molten salt pump mass flow rate [w_{MS}];
- turbine admittance valve [Y_T];
- feedwater general pump mass flow rate [w_{FW}];

- recirculation pump from Separator [w_{SEP}];

The desired controlled variables are:

- mechanical power output [P_{MEC}];
- evaporation pressure [p_{EVA}];
- feedwater OTSG inlet temperature/MS OTSG outlet temperature [T_{FW}];
- separator level [l_{SEP}].

It is worth noticing that when the separator is running wet, the heat exchange within the economizer is very low: the joint effect of pressure reduction and T_{FW} increase due to recirculation strongly reduces the molten salt temperature drop, and so the water temperature increase. Since the fluid temperatures at the economizer cold end are very close, by controlling one of the two temperatures, the other one varies accordingly.

The correct couplings between control and controlled variables is evaluated again through the RGA matrix, which is reported in Tab. 3.3 for the 50% load operating point.

		INPUT			
		Δw_{MS}	ΔY_t	Δw_{FW}	Δw_{sep}
OUTPUT	ΔP_{el}	0.90	0.19	-0.10	0.01
	Δp_{eva}	0.02	0.82	0.00	0.16
	Δl_{sep}	-0.16	-0.01	1.10	0.06
	ΔT_{FW}	0.23	0.00	0.00	0.77

Table 3.3: *RGA coupling at low load*

The proposed couplings seems to be the correct ones, since the matrix is pretty close to the identity matrix. Moreover this trend is the same for 40%, 30% and 20% load, so that the control architecture has not to be changed. The correctness of the proposed pairings has been confirmed also by the analysis of the OTSG portion shown in Fig 3.4. A strong influence between inlet feedwater inlet mass flow, separator recirculated mass flow and separator level has been noticed, resulting in a fast filling of the separator.

By controlling the separator level with feedwater mass flow and feedwater OTSG inlet temperature (T_{FW}) with separator recirculation pump mass flow (w_{SEP}) naturally decouple the system, since no internal mass

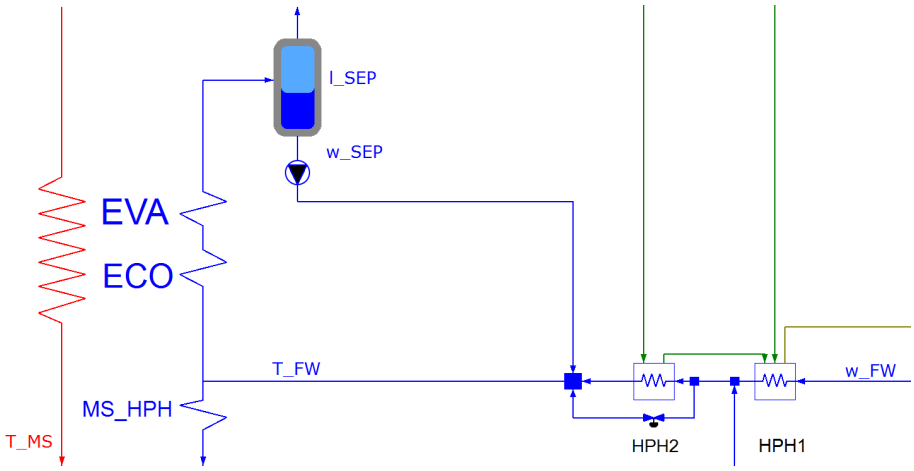

Figure 3.4: *Particular of the recirculation circuit*

flow feedback occurs. For instance, if the recirculated saturated flow is increased, the vapor quality at the evaporator outlet decreases and the separator level increases. The feedwater main pump will react decreasing the feedwater mass flow until the desired separator level is restored, independently from the actual value of recirculated mass flow. Even if it would be more obvious to control the separator level locally with the separator pump and feedwater inlet temperature with feedwater inlet mass flow.

3.5 Controllers tuning

The process to be controlled changes from high to low load, both in terms of the dynamic response of the controlled variables both in the choice of the manipulated variables:

- P_{MEC} change the controller parameters between high load and low load;

- p_{EVA} controller is tuned only at low load while is kept open at high load as it will be discussed later in this section;

- T_{FW} is controlled, at low load, by w_{SEP}, as stated in the previous section, and by θ_{BP} , bypass valve at HPH2, at high load;

- l_{SEP} is controlled, at low load, by w_{SEP}, while is not controlled at high load since separator runs dry;

- dT_{SH} is controlled by w_{FW} at high load while at low load is not controlled (the separator becomes wet, thus steam degree of superheating tends to zero).

The change in the controller parameter for the molten salt mass flow and mechanical power output is confirmed by the Bode diagram of its transfer function. In Fig. 3.5, it is clearly visible that the trend of both magnitude and phase is different between high and low loads groups of lines. This approach allows to achieve a faster response at high load, without having poor performances and introducing oscillations at low loads due to the lower phase in the frequency range of interest (> 0.1 rad/s).

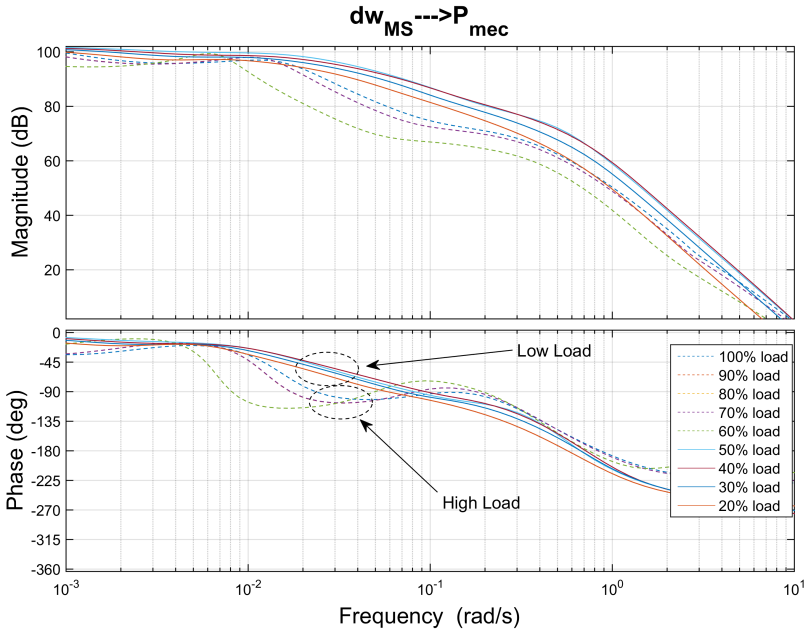

Figure 3.5: *Bode Diagram of the transfer function between molten salt mass flow and mechanical power output*

3.5.1 Feedforward and feedback Control

The **feedforward control (FF)** consists of the definition of the manipulated variables values a priori with regard to another variable, for instance the plant/OTSG load. The control system changes the actuators position without waiting for the process reaction, making the set point tracking faster. This strategy requires a good knowledge and a low uncertainty of the process and the disturbances.

On the other hand, the **feedback control (FB)** defines the control variables values in respect of the gap between the actual and the desired value of the controlled variables. This approach is more effective if the process and its disturbances have a high uncertainty, but could lead to instability.
The following consideration can be made about the process:

1. the heat source is stable and quite easily controllable, while the heat exchange relies on convection mechanism, which has a much lower uncertainty level if compared with radiation mechanism related to combustion;

2. the process itself is not affected by relevant disturbances and is repeatable. This means that, once the dynamic model would be validated through experimental data, it will be substantially close to the actual process.

Thus, in order to achieve good control system performances, the adoption of both FF and FB control strategies seems to be the best solution. In particular:

- the FF control is adopted on all the control variables. The FF signal defines the actuators positions through static maps, whose outputs are a function of the OTSG load, i.e. the plant power output. The maps values could be both the result of an optimization procedure or process bounds. Filters could be applied on the FF signals, in order to improve the performance of the control system, i.e. to reduce the possible overshoots or undershoots;

- the FB control is adopted only when strictly required, basically for safety or plant performance requirements;

3.5.2 Mechanical power control

The mechanical power output is controlled by regulating the hot molten salt pumps both at high and low loads.

The step response of the process transfer function shows a minimum phase behavior with a low phase delay in the bandwidth of interest, so that a PI controller can be used to obtain good crossover frequency both at high and low loads as can be appreciated in Fig. **??**. Table 3.4 shows the controller parameters used at high and low load.

HIGH LOADS TUNING			LOW LOADS TUNING		
K_p	0.0004		K_p	0.000086	
T_i	16	s	T_i	571.4	s
T_d	0	s	T_d	0	s
ω_c	0.1	rad/s	ω_c	0.1	rad/s
ϕ_m	65	°	ϕ_m	75	°

Table 3.4: *The controller parameters for mechanical power at high and low load*

3.5.3 Evaporation Pressure control

The live steam pressure is controlled through the turbine admission valve. In order to prevent the OTSG molten salt outlet temperature from decreasing too much, the minimum allowed pressure is 85 bar. Thus, at low load the pressure control loop is closed, and constant minimum pressure is maintained. As for power control, a PI controller is sufficient to obtain a crossover frequency around 0.1 rad/s (Tab. 3.5 shows contoller parameters and Fig. 3.7 shows the open loop transfer function (L(s)) together with step response).

At high load, the plant runs in sliding pressure mode[1]. There are mainly two kind of sliding pressure mode that can be implemented:

- modified sliding pressure: This mode has a limited amount of pressure throttling to provide a modest amount of fast-response load reserve [20]. It is generally used to provide a first load response for primary frequency control; as a consequence, keeping the valve not completely open reduces cycle efficiency;

- pure sliding pressure mode: this operation does not offer this kind of load or frequency response and is therefore generally not practiced, although in this mode efficiency is not affected.

Since primary control has not been taken into account yet in the control strategy, the evaporation controller at high load is kept in open loop, with admittance valve completely open.

In addition, this configuration is highly different from a coal plant, in which the active control on pressure is used also to compensate thermal inlet fluctuations caused by coal mills.

As discussed early, in pure sliding pressure mode the pressure is imposed by the turbine inlet, explained by taking into account the mass flow

[1] The basic nature of a simple, rotating turbine is to require less pressure as load and flow rate are reduced, and if the main steam pressure is limited to only that required for each load, this mode is referred to as pure sliding pressure. [20]

characteristic equation of a choked turbine:

$$\frac{w\sqrt{T_{IN}}}{p_{IN}} = const$$

Looking at the formula, if steam flow increases (at constant temperature, which is the case considered) also pressure will increase. Substantially pressure is directly proportional to steam flow at high load.

LOW LOADS TUNING		
K_p	-1e-12	
T_i	9.484	s
ω_c	0.1	rad/s
ϕ_m	75	°

Table 3.5: *The controller parameters for pressure at low load*

3.5.4 Feedwater temperature control

Both the crossover frequency at high and low loads of the open-loop transfer function L(s) of the feedwater temperature control could be much higher than 1 rad/s, i.e. the control loop could be quite fast. However, the actual bandwidth will be limited around 0.1-0.2 rad/s by the temperature sensor dynamic, which represents the bottleneck of this temperature control loop, Fig. 3.8.

At high loads, the by-pass valve of the last high pressure pre-heater controls the feedwater temperature. Since the temperature variation across this heat exchanger is significant (75 °C), the resulting mix temperature could be increased until almost 270 °C, so that a good safety margin can be guaranteed. Because of the lower bound of the feedwater inlet temperature is 245 °C, which correspond to the design set point, it is convenient from the efficiency point of view to keep the valve almost fully open at 100% load, and then gradually close it as the OTSG load decreases, until it is completely closed.

At low loads, the recirculated mass flow from the separator controls the feedwater temperature. Again, once the separator is running wet, the heat exchange within the economizer is very low, so that the fluid temperatures at the economizer cold end are very close. This means that by controlling one of the two temperatures, the other one varies accordingly.

A PI controller is sufficient to obtain good control performances, both at high load and low load (Tab. 3.6 and Fig. 3.8).

HIGH LOADS TUNING			LOW LOADS TUNING		
K_p	-7.925e-6		K_p	0.01523	
T_i	0.001	s	T_i	2.267	s
ω_c	0.1-1	rad/s	ω_c	0.1	rad/s
ϕ_m	80-90	°	ϕ_m	90	°

Table 3.6: *The controller parameters for feedwater temperature control at high load (controlled by θ_{BP}) and low load (controlled by w_{SEP})*

3.5.5 Control of the steam degree of superheating

At high load, the steam degree of superheating has to be kept around its nominal set point (20 °C), in order to keep the OTSG temperature profiles as close as possible to their nominal values. In fact this configuration reduces the thermal stresses of the heat exchanger tubesheets at the superheater cold end and EVA2 hot end, see Fig. 3.4. This is done through a fine control of the feedwater mass flow.
Unfortunately, the step response between the feedwater mass flow and the degree of superheating shows a non-minimum phase behavior: when a small increase of mass flow occurs, the degree of superheating initially increases as well (not as expected), and only after some seconds it begins to decrease, as shown in Fig 3.9.

The bandwidth of this closed loop is thus limited at about 0.02 $\frac{rad}{s}$ (see Fig. 3.10 at 60% load) and a simple PI/PID is not enough to guarantee the closed-loop stability within the desired frequency range.
Other controlled variables have been taken into consideration, such as difference between molten salt SH and RH outlet temperature, net heat exchanged through the evaporation section or molten salt temperature in between EVA1 and EVA2 but all of them showed a similar behaviour to the steam degree of superheating response.

Study of the Non-minimum Phase behaviour

The open loop step response of the steam degree of superheating after EVA2 (dT_{SH}) shows a non-minimum phase behaviour, leading to problems in achieving the control objectives. As it has been pointed out, the use of a PI does not permit the achievement of the desired frequency range, thus a more advanced controller that takes into account the intrinsic dynamic response of the system at different load is designed.

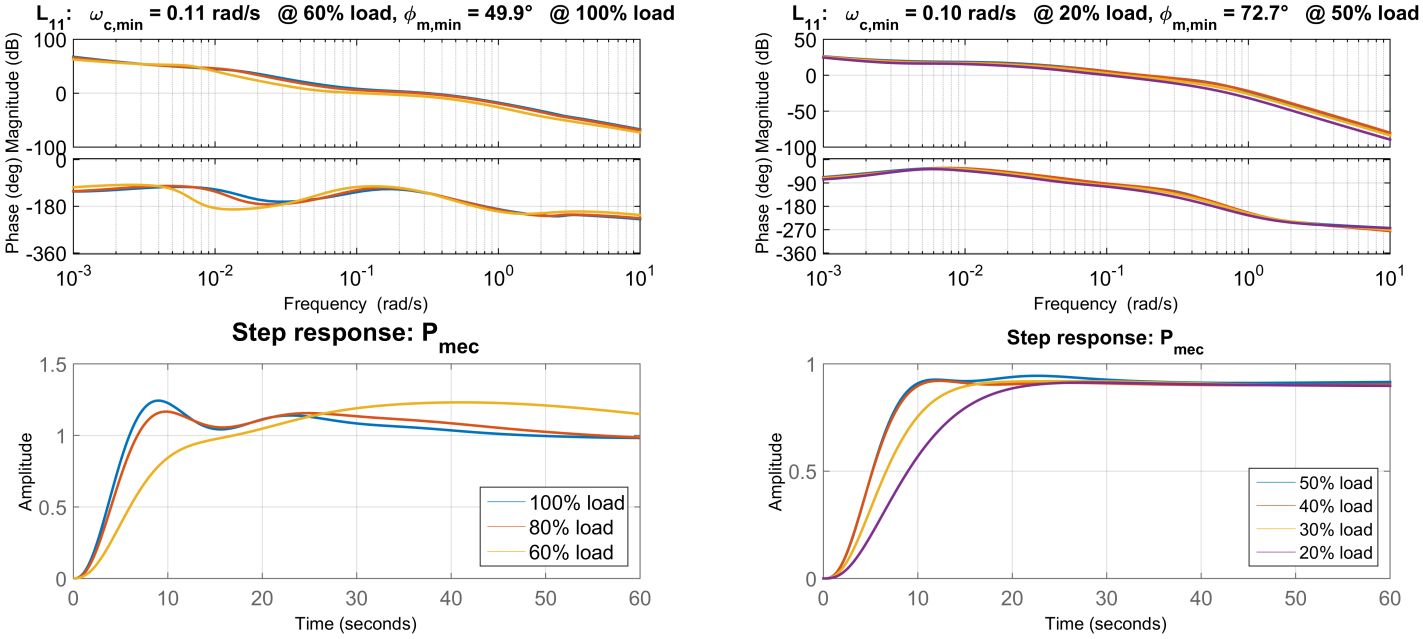

Figure 3.6: *Open-loop transfer function Bode diagram (L(s)) and closed-loop step response (set point tracking) of the Mechanical Power at high and low load*

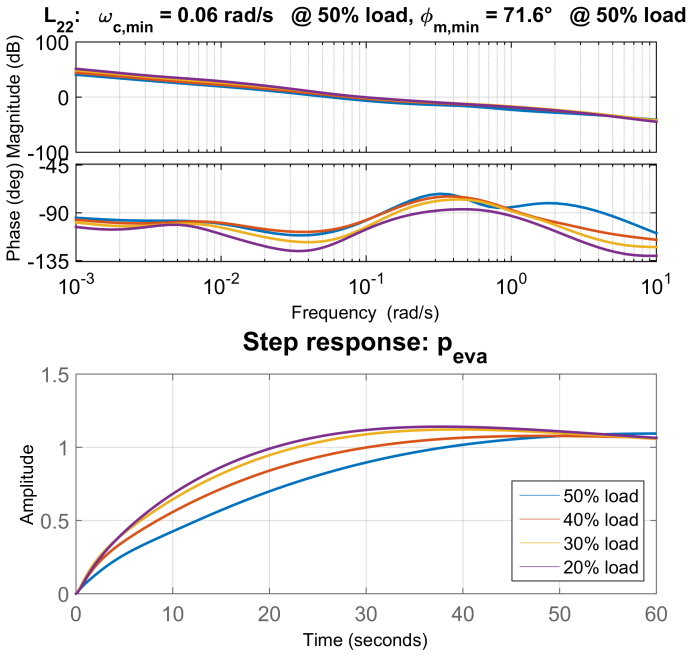

Figure 3.7: *Open-loop transfer function Bode diagram (L(s)) and closed-loop step response (set point tracking) of the Evaporation Pressure control at low load*

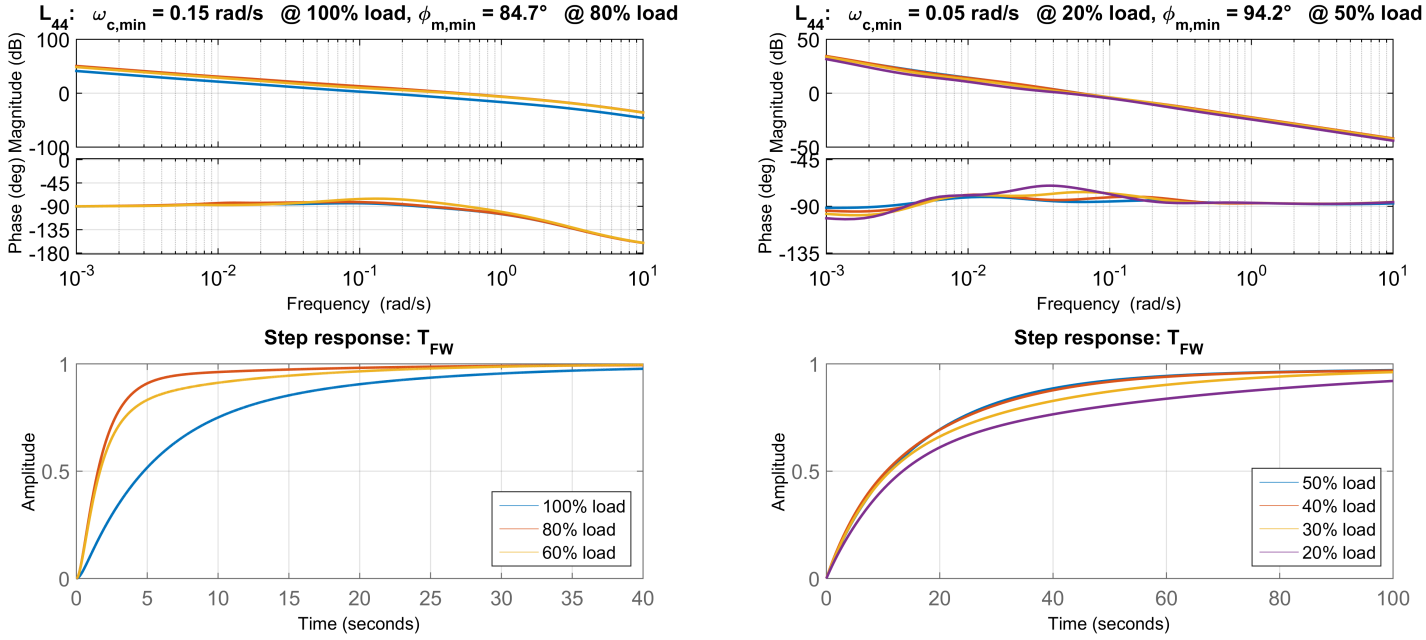

Figure 3.8: *Open-loop transfer function Bode diagram and closed-loop step response (set point tracking) of the Feedwater Temperature control at high load, controlled by θ_{BP}, and at low load, controlled by w_{SEP}*

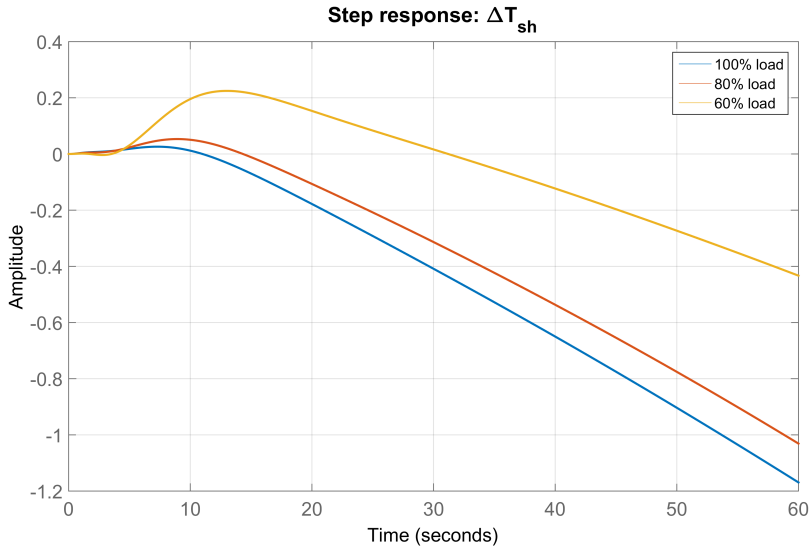

Figure 3.9: *Step response of the open-loop transfer function between w_{FW} and ΔT_{SH}*

For a detailed description of non-minimum phase systems see Appendix A. The first step made to study the transfer function between feedwater and dT_{SH} has been to reduce the linearized system, in order to see the right half plane zeros (RHPZ) that affect the dynamic of the system in the range of frequency which are of interest for control (from 10^{-3} to 10^{0}).

The linearized systems exported from Dymola consist of state space models with about 180 states. This put some limitations in the determination of which zeros and poles effectively act on the dynamic of the system and which are unobservable or uncontrollable. Hence, model reduction techniques have been applied.
Steps performed to study the system have been:

Balanced Realization of the system: a new state-space description is obtained so that the reachability and observability gramians are diagonalized. This defines a new set of invariant parameters known as Hankel singular values. This approach plays a major role in model reduction which will be highlighted in this chapter. [18]
The Hankel singular values of a stable system indicate the respective state energy of the system. Hence, the reduced order can be directly determined by examining those values.

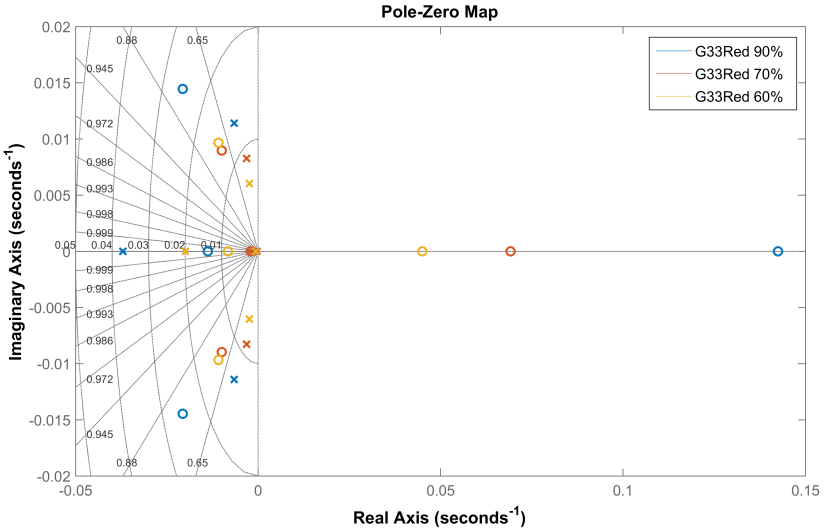

Figure 3.10: *90%, 70% and 60% load map of zeros and poles, where is observable the RHP zero moving towards zero, thus increasing the inverse response*

Model order reduction: models have been reduced using one of the Model reduction routines provided by Matlab specifying an error bound between system reduced and the original system; this function eliminates also uncontrollable or unobservable states in state-space models, and cancels stable pole-zero pairs in transfer functions [16].

Reduced order models are all in the range of 9 to 11 states, which is a pretty good result compared with the original system.

A study of the poles and zeros of the reduced system reveals the presence of a RHP zero and three pairs of poles and zeros in the LHP as can be seen in Fig. 3.10

Feedback Control Design of Non-Minimum Phase system

After observing the behaviour of the non-minimum phase system through the analisys of poles and zeros, a simple, yet effective, control design architecture has been proposed.

The main idea is the inversion of the dynamics of the system, changing the sign of the RHP zero in order to have a stable controller, and the addition of a gain and an integrator to obtain zero steady state error. The design is taking into account the dynamic response at 60% of load, because shows

the highest delay.

The controller has the following form:

$$R_{33} = -\frac{0.0003}{s}\frac{(s+0.01993)(s+0.0006302)(s^2+0.004837*s+4.222e-05)}{(s+0.04501)(s+0.008267)(s^2+0.02172*s+0.0002116)} \quad (3.1)$$

and Fig. 3.11 shows the results of the closed loop system at different load calculated on the linearized systems at 100%, 80% and 60% load.

3.5.6 Separator level control

At low load operation, the feedwater main pump controls the separator level. Since the separator size is quite small, the control level has to be fast enough to avoid the complete filling or emptying of this device. A PI controller permit a crossover frequency of 0.08 rad/s, that can be considered enough for the requested performance.

The controller parameters are:

K_p	15.73	
T_i	50	s
ω_c	0.1	rad/s
ϕ_m	54-60	°

3.6 High-low load transition

Transition to low load operation is done at a pre-defined load. In low load recirculation starts being needed to keep sufficiently high feedwater temperature and/or sufficiently high molten salt outlet temperature (currently identified around 55% load). Transition to low load operation involves manipulation of the heat exchange profile to enter in the two-phase zone at the evaporator outlet.

As a baseline, the transition takes place as follows:

- Regulation of feedwater flow is switched to separator level control;
- Feedwater flow is temporarily increased to fill the separator;
- When a sufficient level is reached in the Separator, separator recirculation pumps are started in order to gradually disable heat exchange into the economizer and transition to low load operation.

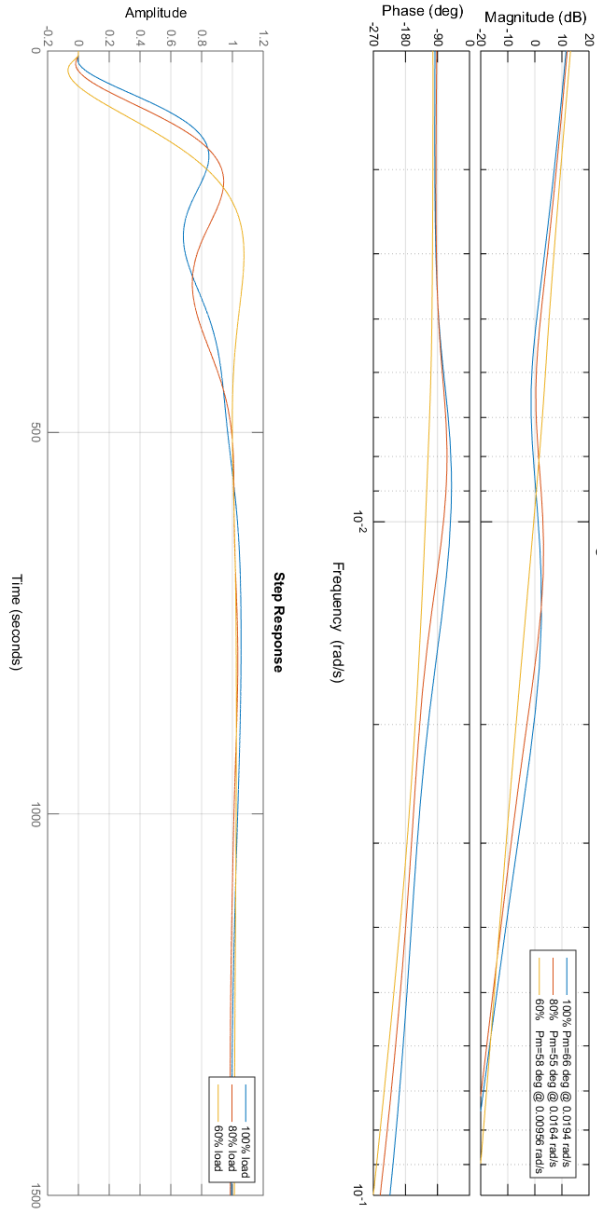

Figure 3.11: *Open loop bode plot and step response of the steam degree of superheating controller*

Transition to high load operation is done at a pre-defined load at which recirculation is not needed to keep sufficiently high feedwater temperature and/or sufficiently high molten salt outlet temperature (reference value about 55% load).
Transition to high load operation involves manipulation of the heat exchange profile to obtain superheated steam at the Evaporator outlet.

As a baseline, the transition takes place as follows:

- Separator level is brought at the minimum value;
- Separator recirculation pumps are shut-down, which allows to "re-enable" the heat exchange surface of the economizer;
- Water in the separator slowly evaporates as it gets in contact with superheated steam coming from
- The evaporator and Separator gradually empties as high load operation proceeds.

In the next chapter, will be presented the implementation of the control strategy presented here on the non linear plant, evaluating the performance of the controllers on realistc scenarios, such as dispatchability request and hot startup ramp, toghether with a preliminary study on the primary frequency control using this architecture.

CHAPTER 4

Study of Decentralized control system in realistic operational modes

In this chapter the implementation of the control strategy presented in the previous chapters is discussed. The reference realistic operational modes are taken from the request of the project.

Dispatchability: the Grid Code is a document delivered of subscript by the transmission system operator (TSO) of every country, which defines the parameters a facility connected to a public electric network has to meet to ensure safe, secure and economic proper functioning of the electric system. It contains also the specifications on the rate of load the plant has to comply, as a function of the amount of power produced. Taking the Italian Grid Code as reference (but also the South african Grid Code [17], where the system could be installed), this plant has to be able to satisfy a ramp of +-10MW in 15 minutes from all the of operating points permitted by the plant (from 20% to 100% of load).

Warm startup: it brings the system from 20% of load to 100% of load, as presented in chapter 2. This ramp is steeper than the dispatchability request, since the demand is to pass from 20% of load to 100% of load

in less than 10 minutes.

Primary frequency control, preliminary study: one of the control strategy targets of this plant is also to permit primary frequency control, i.e. fast yet small variations of the power from the reference signal to stabilize frequency in the network. This requirement is present in the grid code and for Italy is requested a variation of +-3% in 15 sec to be maintained for at least two minutes on Power reference signal.

4.1 Control Unit in the simulation environment

Connected to the rest of the plant through a SignalBus, this Unit receives as input all the actual values of the variables to be controlled and has as output the controlled variables.

As a basic component, this unit uses the controllers of the IndustrialControlSystems library, developed by Marco Bonvini and has been presented at the 9th Modelica conference, held in Munich 3-5 September 2012 [4].

The general structure of a control loop is as follows and it comprehends the following general parts:

- the controller (PI, PID);
- the FeedForward tables;
- the SetPoint tables;
- the actuator dynamic, modeled as a first order low-pass transfer function for pumps and valves, with a time constant of 2 s and 0.3 s respectively.

4.1.1 Additions to the control system for the implementation

In addition to the tuning of the controllers some additions are mandatory to test the strategy on the non linear system presented as follows:

Feedforward tables: useful to allow a faster response of the manipulated variables as the load changes as discussed in Chap. 3.5.1, with the feedback action operating to achieve zero steady state error;

Saturations and Anti wind-up feature in the actual system, actuator limits and anti-windup play a crucial role, so they have to be correctly reproduced in simulation;

Tracking mode: in order to switch from Low load to high load and viceversa, since on every manipulated variable acts two controllers, it is important to take care of the transition from one configuration to the other in a bumpless way. This feature was already implemented in the controllers of the IndustrialControlSystems library [4] and it has been used. While a controller is active, the other one is set in tracking

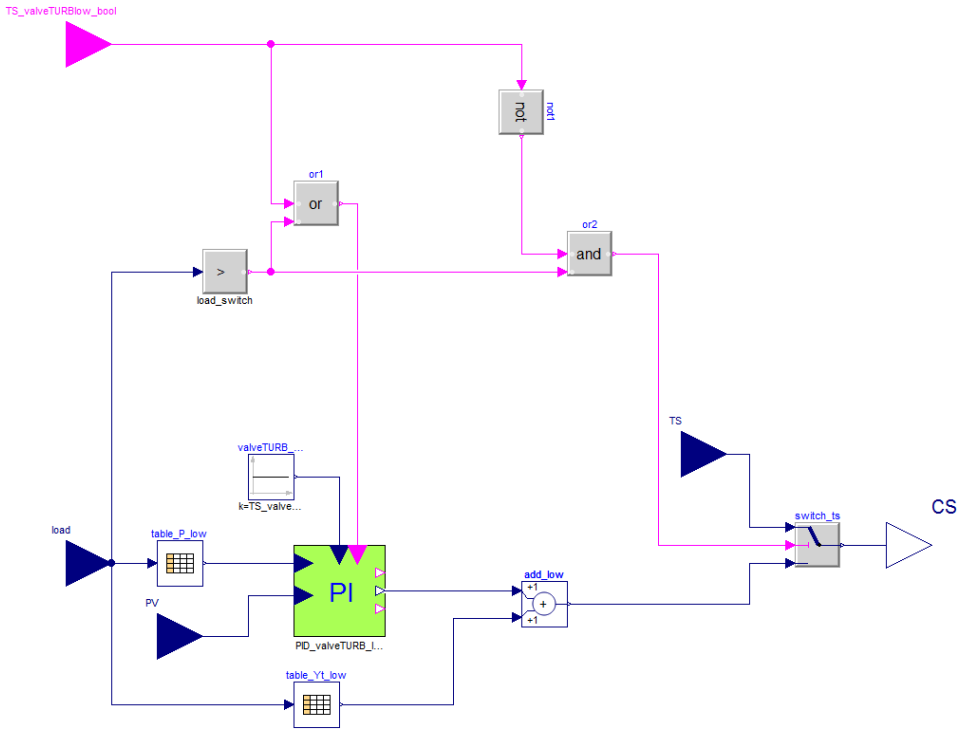

Figure 4.1: *Controller architecture with feedforward tables, tracking signal (that activate the controller) and switch between low and high controller (to allow a bumpless transition between the two controllers); saturations and anti-windup features are inside the PI block*

mode, which means that the control signal exiting the non-active controller is exactly the control signal of the active controller. When the switch is trigged (by, for instance, the passage from high to low load) the new controller manipulated variable starts exactly from where the other controller has computed (Fig. 4.1);

Reference signal: the reference signal given to the controllers is ramp like but with the nose and tail of every ramp smoothed. This decision is sustained by the fact that, for dispatchability, is not taken into consideration the trajectory followed to move from a certain load to another,

but only the starting and the arrival point of it. Thus, a smoother ramp is preferred to reduce stress that could arise from the sudden change in the ramp rate;

Addition of static decoupler between w_{MS} and w_{FW} since a coupling effect has been noticed between w_{MS} and w_{FW}, a static decoupler is designed. In order not to change the tuning of the controllers a backward decoupler is used, using the following formulas to calculate the gains (backward decoupler diagram is showed in Fig. 4.2):

$$\Gamma_{21} = \frac{P_{21}(s)}{P_{22}(s)}; \qquad \Gamma_{12} = \frac{P_{12}(s)}{P_{11}(s)};$$

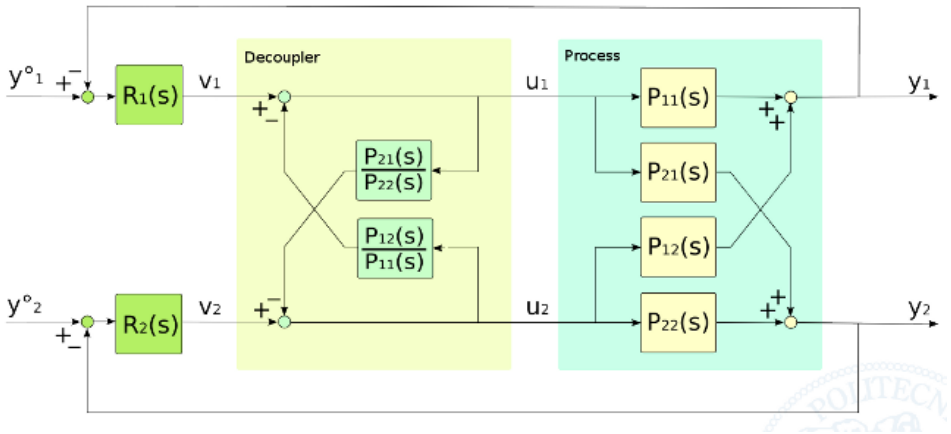

Figure 4.2: *Backward decoupler, image courtesy of IndustrialControlSystems wiki [4]*

4.2 Dispatchability

Three simulation results are presented here, as an example of the three different cases to show the behaviour of the control system on the non-linear model:

- Simulation at low load, transition from 30% to 40% of load, Fig. 4.3;
- Simulation at high load, transition from 70% to 80% of load, Fig. 4.4 ;
- Transition from low to high load, transition from 50% to 60% of load, Fig. 4.5;

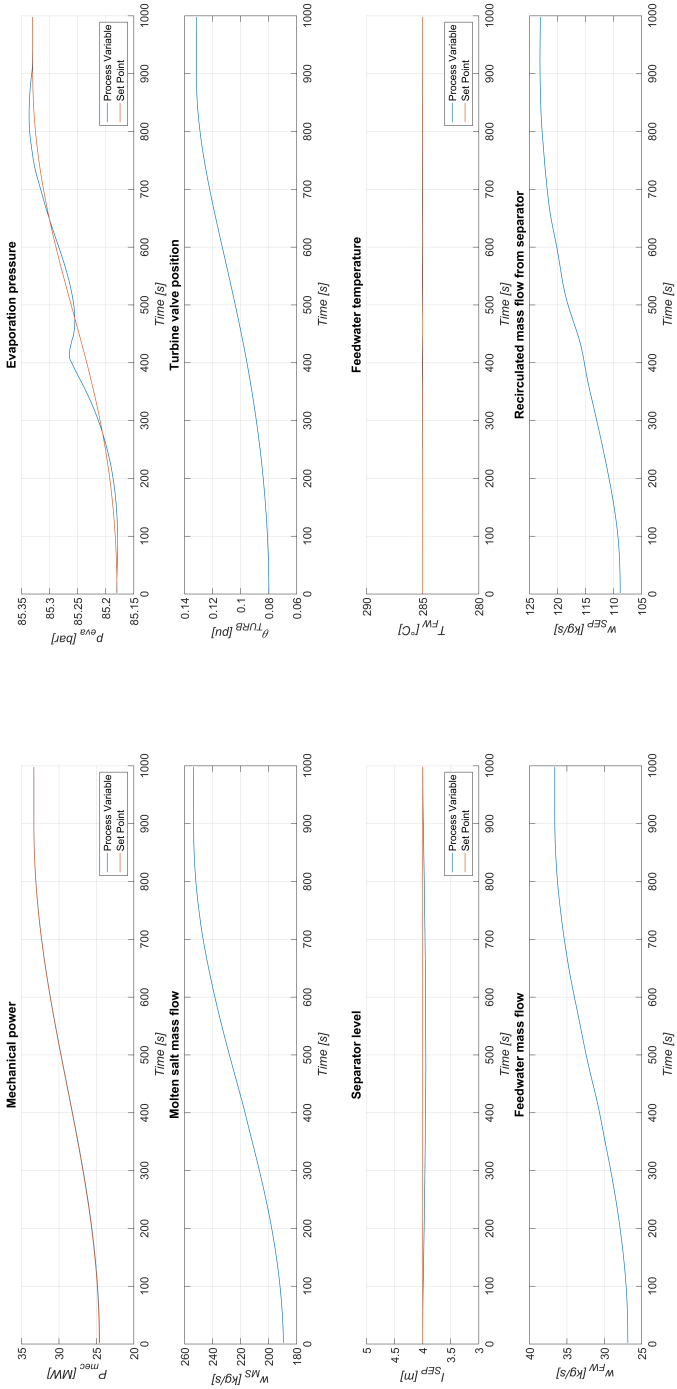

Figure 4.3: *Dispatchability at low load: 30-40% ramp in 15 min, 900 sec. Separator is filled.*

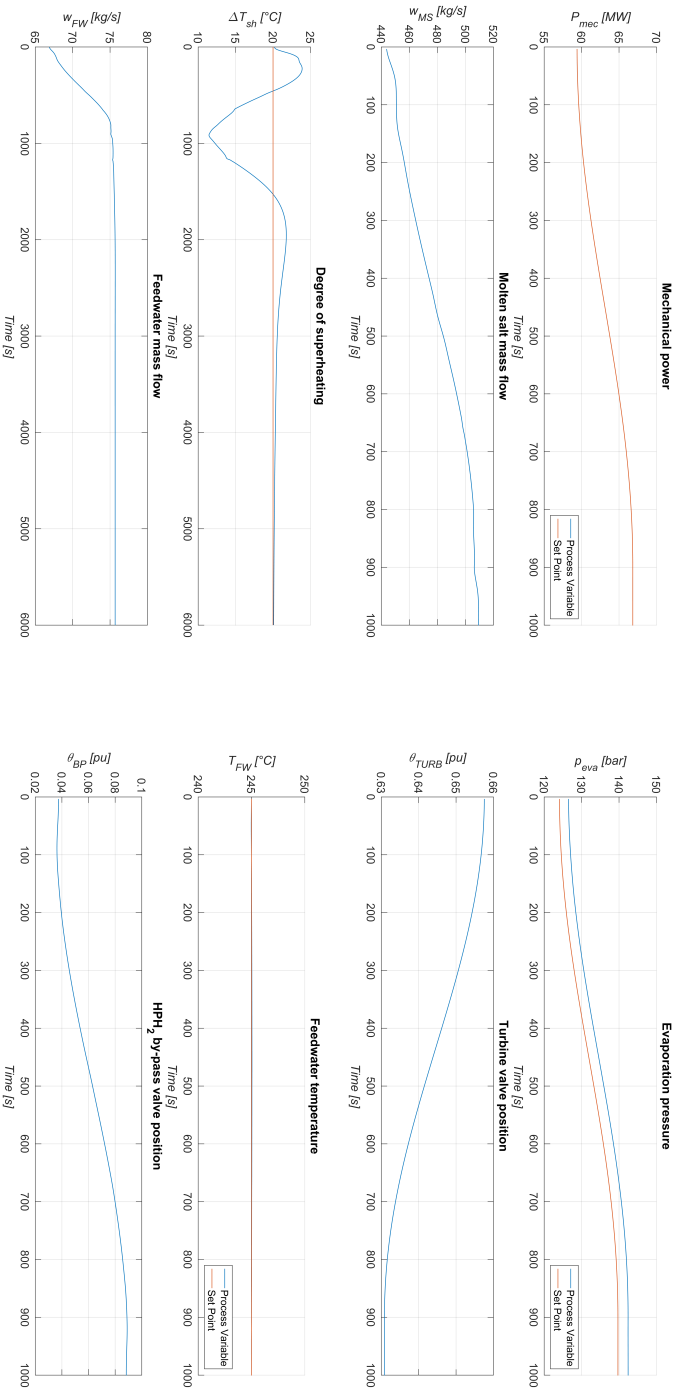

Figure 4.4: *Dispatchability at high load: 70-80% ramp in 15 min, 900 sec. Steam degree of superheating is controlled*

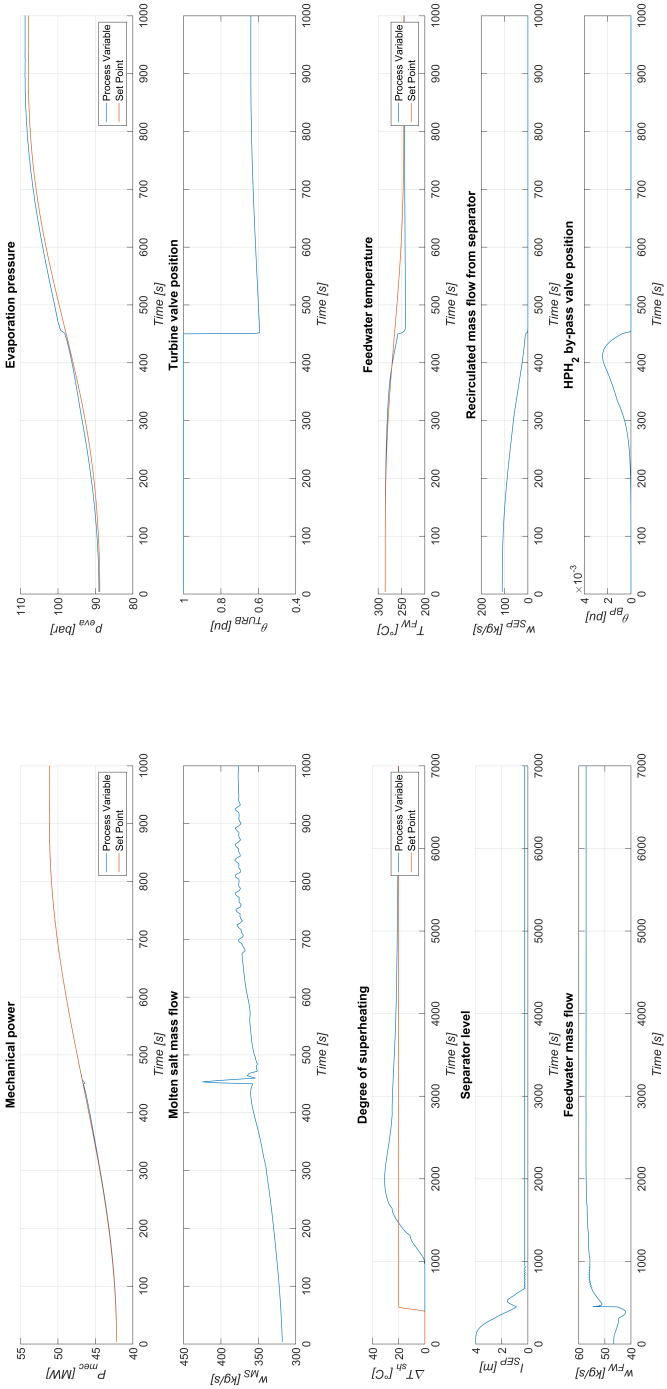

Figure 4.5: *Dispatchability at transition load: 50-60% ramp in 15 min, 900 sec. Switch between low and high load control strategy*

It is worth to be noticed that, since only the high pressure part of the plant is simulated, the setpoint of power refers only to the high pressure and medium pressure section of the turbine, but simulations performed on the entire plant shows a similar dynamic behaviour, with the offset on the power produced being the only noticeable difference. During all the tests presented here the dispatchability request (i.e. the power reference tracking) is satisfied, together with the control of the other variables taken into account in the control strategy. The only drawback that can be noted, although not relevant from the performance point of view, is the delay of steam degree of superheating during the passage from low to high load (see Fig. 4.5).

4.3 Warm Startup

As can be seen in Fig. 4.6, the system is able to manage the warm startup without stressing too much the manipulated variables while keeping the controlled variables relatively close to the reference signals. At the end of the ramp there is a little transient and the controllers acts to have zero steady state error. This fact can be explained taking into account that, in this simulation, the predominant part in the control action is given by the feedforward tables while the closed loop control acts at the end of the ramp.

4.4 Primary frequency control, preliminary study

There are many control strategies that can be implemented, in order to have a fast response on a variation of the reference signal, many of them in open loop while others in closed loop.
One possible choice is to close the steam extractions from turbine stages, acting in open loop, in order to have a sudden increase in Power production. Since this increase does not hold for a long period it is important to support it with a closed loop control strategy, in order to satisfy the grid code requirement. In this chapter a ramp like transition of 10MW in one minute on the power reference is studied (with the other reference signals as function of the load). The simulations verify how fast and robust the designed control system can be to guarantee this variation and satisfy the control objectives.

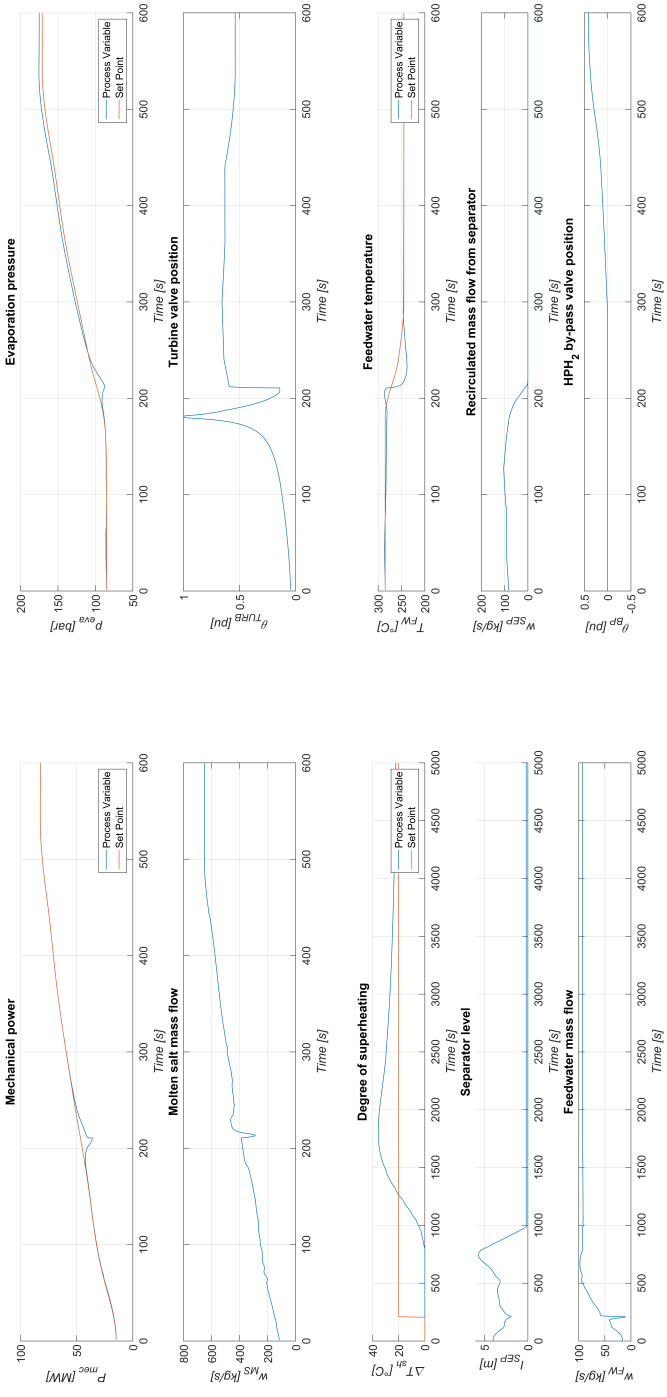

Figure 4.6: *Startup plant, passage from 20 to 100% load ramp in less than 10 minutes (540 sec).*

As presented for the dispatchability request, three simulation results are presented here:

- Simulation at low load, transition from 30% to 40% of load, Fig. 4.7;
- Simulation at high load, transition from 70% to 80% of load, Fig. 4.8;
- Transition from low to high load, transition from 50% to 60% of load, Fig. 4.9.

4.4.1 Simulation results

The simulations performed here are for a variation of +-10MW/min on the power reference, starting from different loads. It can be noted that, at high load, the controller degrades at loads around 60%, especially on the steam degree of superheating where the delays in the non minimum phase system becomes greater.
Also the transition between low to high load can be improved (e.g. there is a loss of power and a noticeable delay in the power responce), while simulation at low load shows good performance.

Fig. 4.10 presents the differences before and after using the static decoupler during the 70-80% ramp performed in 1 minute. As can be noticed, although seems that with the static decoupler the action on the manipulated variables is more relevant, the set point tracking performances improve, since the power tracking is faster and the peaks on the steam degree of superheating control are smaller in magnitude.

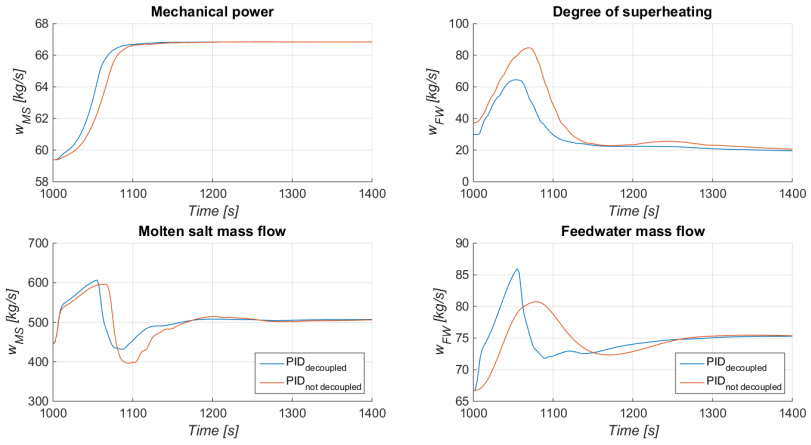

Figure 4.10: *Behaviour of the power and steam degree of superheating controllers with and without backward decoupler between w_{MS} and w_{FW}*

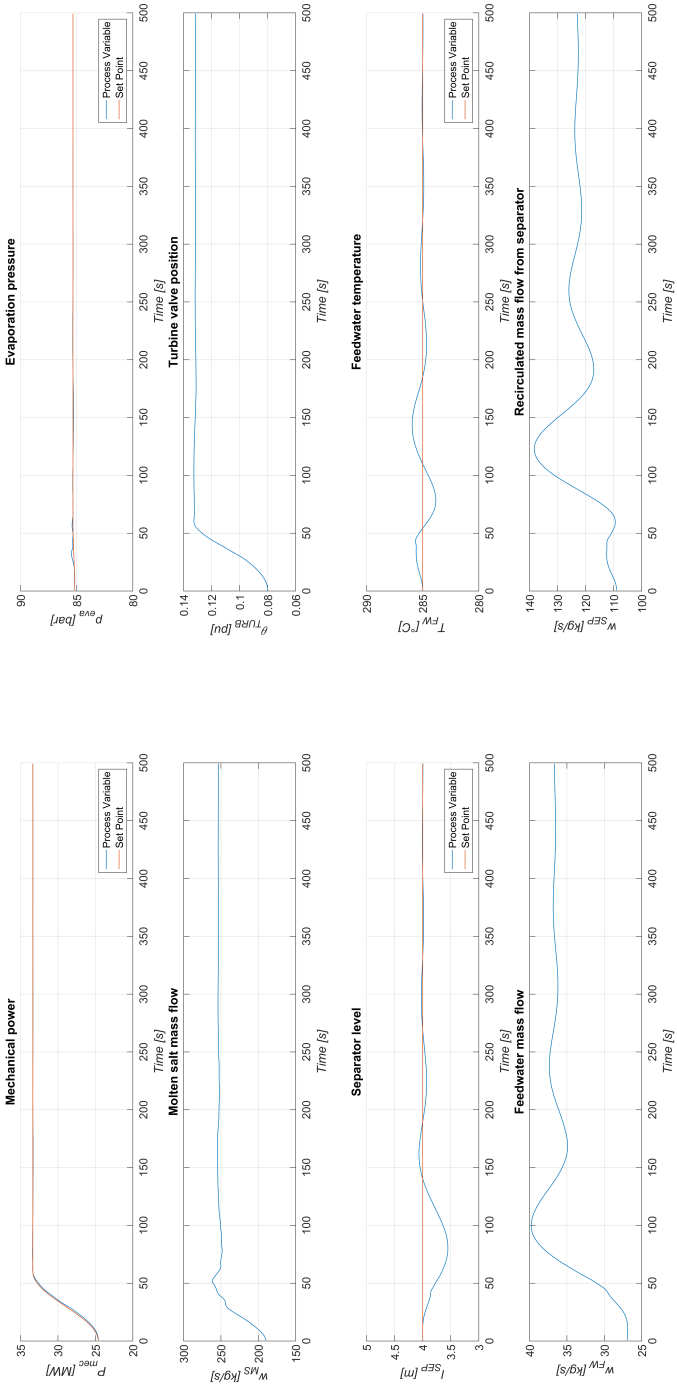

Figure 4.7: *Preliminary primary control at low load: 30-40% ramp in 1 min. Separator is filled.*

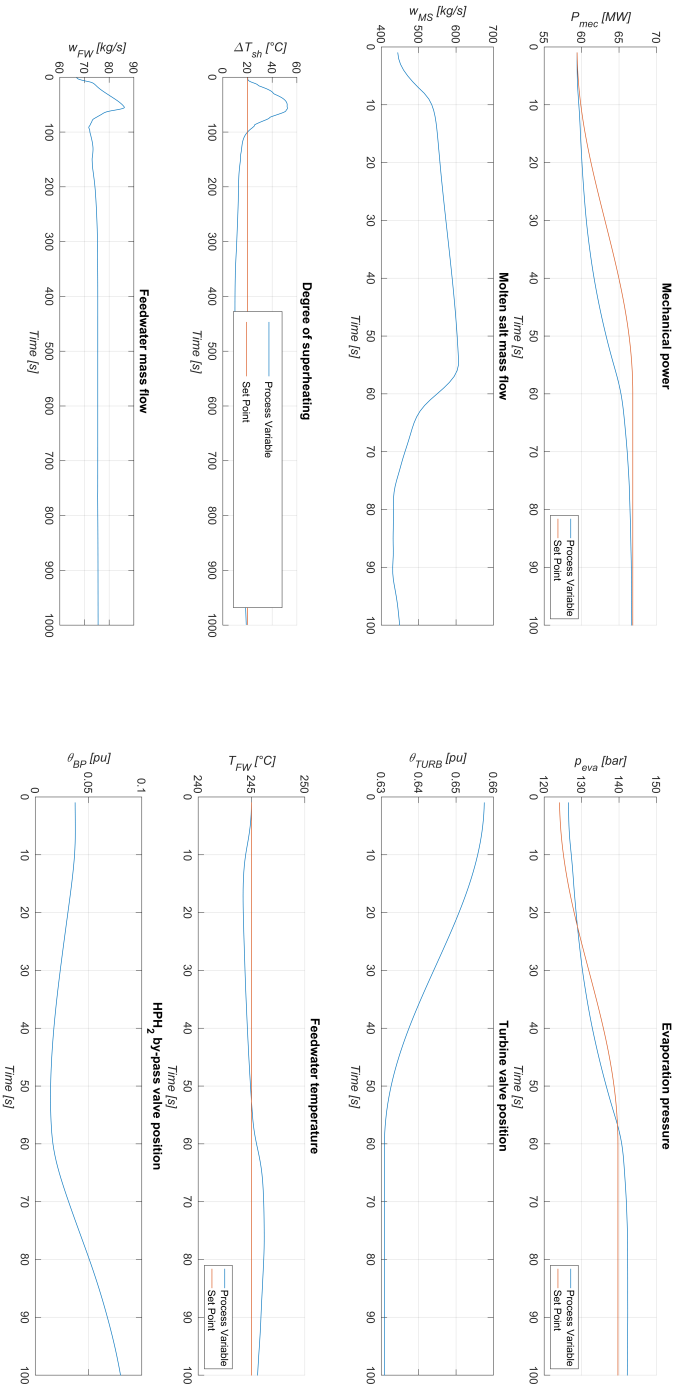

Figure 4.8: *Preliminary primary control at high load: 70-80% ramp in 1 min. Steam degree of superheating is controlled*

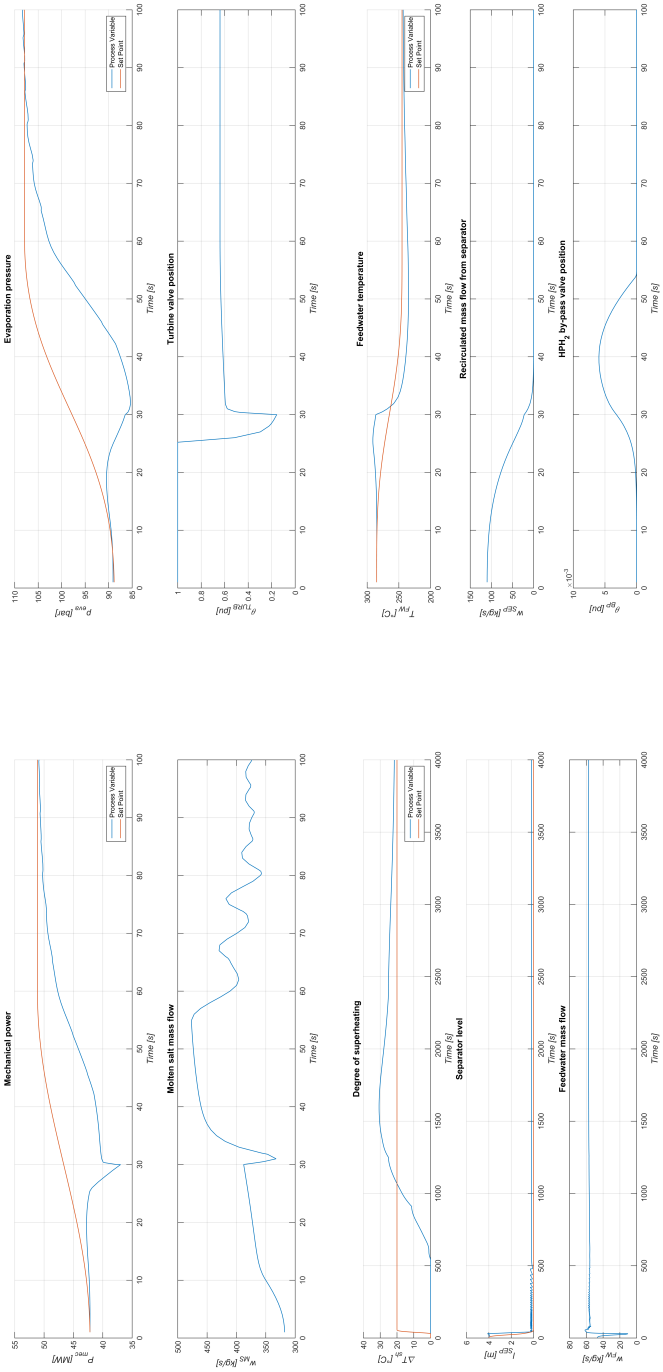

Figure 4.9: *Preliminary primary control at transition load: 50-60% ramp in 1 min. Switch between low and high load control strategy*

4.4.2 Remarks on simulations results

As presented in this chapter, a decentralized control strategy has limited capabilities in respect to a centralized control strategy when performance and robustness are key factors. As an example, the steam degree of superheating in the 70-80% transition (see Fig. 4.8) nominal value of almost 30 degrees, which could be too much, on a long period, in terms of thermo-mechanical stress on the heat exchanger tubesheets.
In the next chapter a centralized control strategy will be discussed and implemented and results are given in terms of robustness, limited action on manipulated variables and performance.

CHAPTER 5

MPC control of plant at high load

In this Chapter the possibility to adopt an alternative centralized control strategy for the OTSG power plant is discussed. The decentralized control system presented in Chapter 3 responds appropriately to the dispatchability requirements, in a 15 minutes timeframe. The starting question addressed by this study is whether the PID control system is still suitable for a lower frame of time (e.g. 1 to 5 minutes) or if it is more convenient to design a centralized control system with improved performances for this specific OTSG power plant, i.e., a control system that:

(a) is responsive;

(b) does not apply excessive variations on the manipulated variables;

(c) is able to regulate the steam degree of superheating in a more robust way.

In this scenario, the centralized control strategy is expected to guarantee the above-mentioned better performances.

The new controller has been designed by means of advanced control strategies. In particular, the approach of Model Predictive Control (MPC) is used. The MPC is based on the use of a model for the prediction of

the outputs of the process to a given reference trajectory and on an on-line optimization process, that requires considerable computational resources. In the past two decades, it has successfully been applied to the control of chemical and industrial plants, thanks to its capability to deal in an optimal form with input/output process limitations (for instance, upper or lower bounds for a specific variable).

As a starting point, the following case is investigated: Linear MPC (LMPC) for the control of the ramp-up/down of the plant with the ramp rate requirement of 10 MW/min. The linear model was derived from the complete non-linear model of the OTSG, in the same way as it has been described for the linear analysis discussed in Chapter 3. Only the control on the feed-water temperature by the by-pass valve on HPH2 was preserved because it acts locally and it does not affect the other outputs considered in this study.

The objective of the LMPC study is to evaluate the improvement on the control performance of the MPC controller, compared to a base control strategy. This approach can be a starting point in order to consider the adoption of a more complex and accurate control system, as Non-linear MPC (NMPC).

A diagram of the centralized LMPC system is shown in Fig. 5.1.

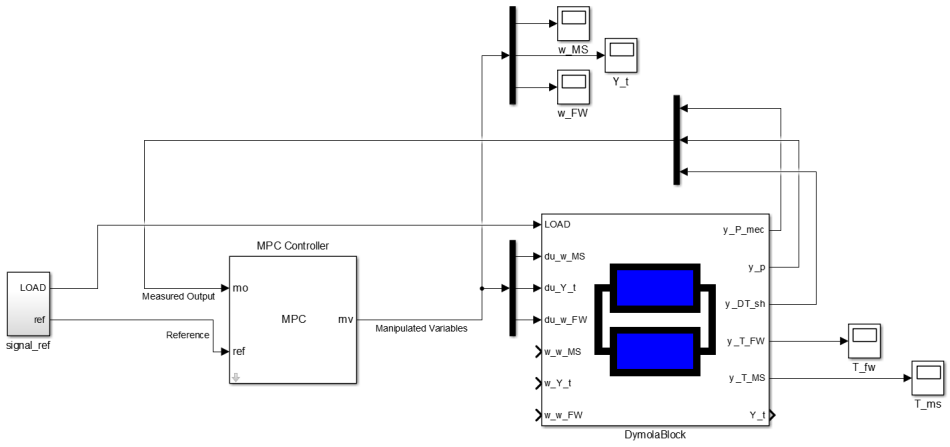

Figure 5.1: *Diagram of the centralized linear MPC*

5.1 Linear MPC implementation

The first target of the Linear MPC control strategy implemented here is to control produced Power, Pressure and steam degree of superheating acting on the molten salt mass flow (w_{MS}), the opening of the turbine valve (Y_t) and the flow of feedwater entering the system (w_{FW}).

5.1.1 Description of Input and Outputs

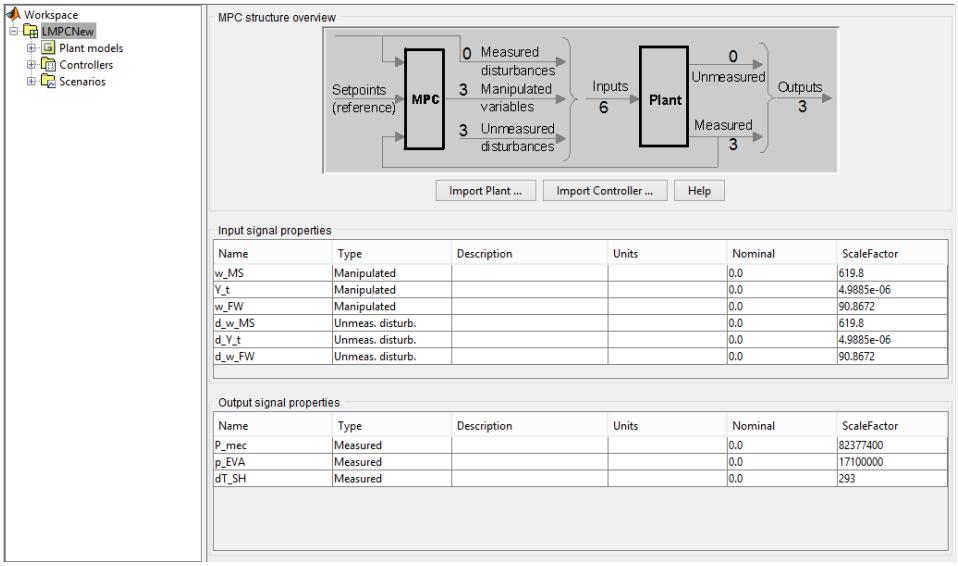

Figure 5.2: *I/O description of MPC*

The linear system has three inputs and three outputs, plus three additional inputs (one signal which sums to every input) used to excite the system with additional noise. This is important in order to implement and tune the Kalman filter (i.e. to update the state estimation) as can be seen in fig. 5.2.

5.1.2 Model Order Reduction

To reduce the order of the system the Hankel singular value decomposition has been used: since the order of the system is high, the number of the states of the linear system exported by Dymola (i.e. the dimension of the matrix A) can be unnecessarily high for the purposes of the controller design. The aim of the reduction is to minimize the number of states of the system to only the significant ones who contribute to the dynamic response

of the I/O model. Retrieving a reduced order system is important to subsequently have a model of lower complexity, easier to handle, especially during advanced control design.
Hankel singular value decomposition is used to study the states that actually contribute to the input/output behaviour as discussed in Sec. 3.5.5 and as presented in Fig. 5.4 It is important, however, to verify the accuracy (i.e. the model mismatch) of the reduced system and compare it with the behaviour of the system at a different load.
The reduced order model linearized at 80% load is compared with the linearized model at 100% and 60% (see Fig.5.3) to observe:

- the model mismatch between the reduced model and the complete 80% model (unreduced);

- the dynamic behaviour mismatch between system at 80% and system at full load or at minimum load (60%, in this study).

It can be noticed in Fig. 5.3 that the reduced model (dotted line) follows the complete 80% model (red line) in the bandwidth of interest (around $10^{-2}\frac{rad}{s}$). The figure shows also the Bode plot of the complete system at 100% and 60% load, which present a similar trend but respectively in advance or delayed with respect to the reduced system. This is important to mention, since by the simulations it will be clear if the choice of using the linearized model at 80% of load has been accurate or not.

5.1.3 Discretization

The reduced model has been discretized in order to use it inside the optimizer. The method used to discretize the model is Tustin's, which is the most accurate method, although it is necessary to check that in the transformation from Laplace domain to discrete domain artificial and poorly dumped oscillatory modes are not introduced. Other methods could have been used as well, such as Backwards Euler which however is less accurate.

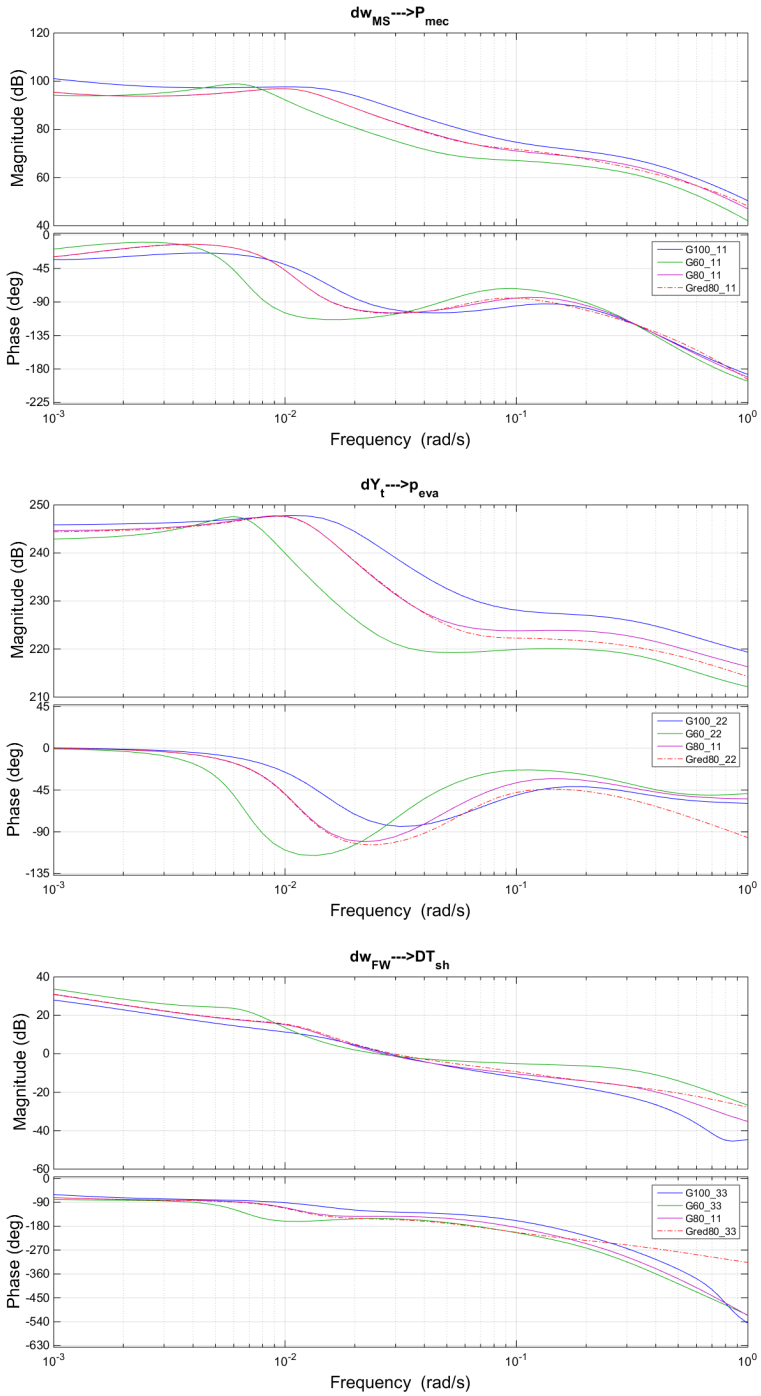

Figure 5.3: *Bode plots of G11-G22-G33 for 100-80-60% linearized systems and 80% reduced system*

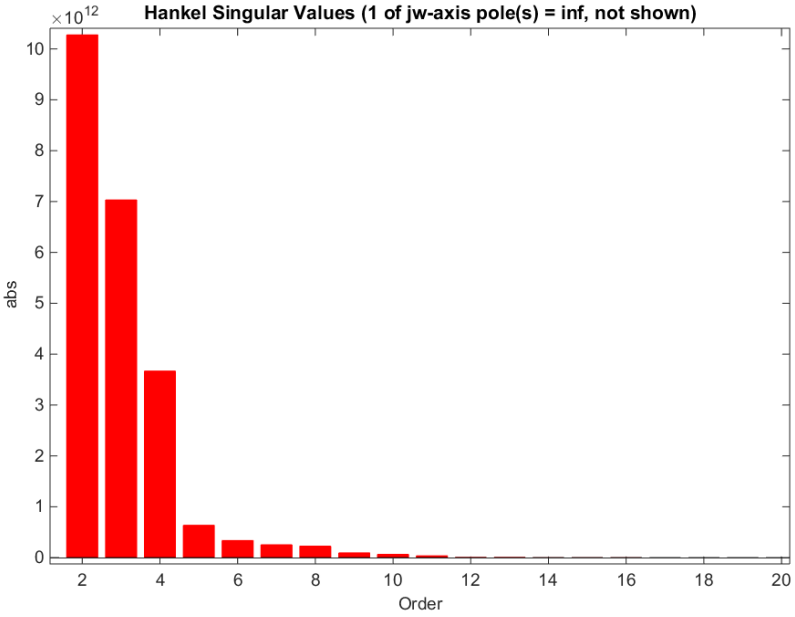

Figure 5.4: *Hankel singular values, after the 12th order the contribution to the input/output behaviour can be neglected*

5.1.4 Control Design

Many tools are available to implement the Linear MPC strategy, being a widely used control technique. For this study the MPCtoolbox from Matlab has been used [17]. The use of already available toolboxes allows to focus more on the design of the controller rather than deal with the implementation of the control strategy which was not a key aspect of this study.

The control design has been split in different phases, summarized as follows:

Import of the reduced, linearized and discretized plant for prediction;

Choice of input and output types: as stated before, the model is characterised by three manipulated inputs, three unmeasured disturbances (noise on input for the Kalman filter) and three measured outputs (Fig. 5.2);

Normalization of the variables: this phase is of utmost importance since the signals used span on a very wide range of decades, from 10^{-6} (Y_t)

to 10^6 (P_{mec} and p_{eva}) thus avoiding it might create problems in the matrix calculations;

Tuning of the Kalman filter: white noise has been added on outputs and step-like noise on inputs (i.e. white noise filtered through an integrator). Also the magnitude of noise has been set accordingly to allow best fit of the predicted model on the actual model;

Prediction Horizon: As for the Prediction Horizon a value of 150 samples has been used. This value directly corresponds to seconds (since the sampling time is 1 s) and it was chosen because it is three times higher than the longest delay of the system, that corresponds to the response of the steam degree of superheating which, at 60% load, shows a delay in open loop of approximately 40 seconds;

Control Horizon: For the Control Horizon a value of 10 samples has been used (10 seconds forward), meaning that, after 10 control action computations made in a optimization step, the control action becomes constant. In a receding horizon control strategy at every step only the first control action is used and then the optimization procedure is performed again. In order not to overload the optimization problem a value that is approximately 10% of the prediction horizon is reasonable;

Choice of the cost function weights, bounds and constraints: upper bounds have been set for maximum and minimum flow of molten salt, feedwater and valve admittance. The weights that appear in the cost function have been set as follows.

- **Input weights:** for each Manipulated Variable a positive Rate Weight has been added, which penalizes the derivative of the MV. Not setting it would cause sudden changes in the input variations;
- **Output weights:** in order to have a faster response, the highest weight has been assigned to Power output; a high weight has also been assigned to the steam degree of superheating because, as discussed in Sec. 3.5.5, it is very important to keep it as close as possible to its setpoint. The pressure has a lower weight because, since at high load the plant runs under the sliding pressure principle as discussed in chapter 3, a faster response would had downgraded the robustness on the dT_{SH} control;

5.1.5 Selected design parameters

In order to fulfill the control objectives described above, multiple sets of design parameters have been tried iteratively. This procedure converged to the choice of the values in Tab. 5.5 whose effectiveness has been proven on the simulation scenarios described below.

Input weights

Name	Description	Units	Weight	Rate Weight
w_MS	Molten salt mass flow rate	kg/s	0	8
Y_t	Admittance valve		0	10
w_FW	Feedwater mass flow rate	kg/s	0	2

Output weights

Name	Description	Units	Weight
P_mec	Power	MW	20
p_eva	pressure	bar	3
dT_SH	steam degree of superheating	°C	15

Figure 5.5: *Linear MPC design parameters*

5.1.6 Setup of simulation Scenario

The MPC controller designed with the Toolbox has been tested on the full dimension, continuous-time linear systems at different loads (100%, 90%, 80%, 70%, 60%) in order to verify the performances of the control architecture and to explore different alternative designs. Three increasingly realistic scenarios have been considered:

Scenario Tab inside MPCTool: This tool consists of a very simple setup, useful to iteratively test different control parameters, such as changes in horizons, limits in control and weights on manipulated and measured variables; a comparison of scenarios related to the different linearized systems (using the controller tuned with the final design parameters) is presented in Fig. 5.6);

Simulink with MPC Controller and state-space linear model: This setup is a step closer to real system implementation, giving the possibility to change reference signals (e.g., ramp-like steps) and interface the MPC controller with the linear state space system in the Simulink environment;

Simulink with MPC Controller and DymolaBlock This setup has been the real benchmark for the validation of the designed MPC controller

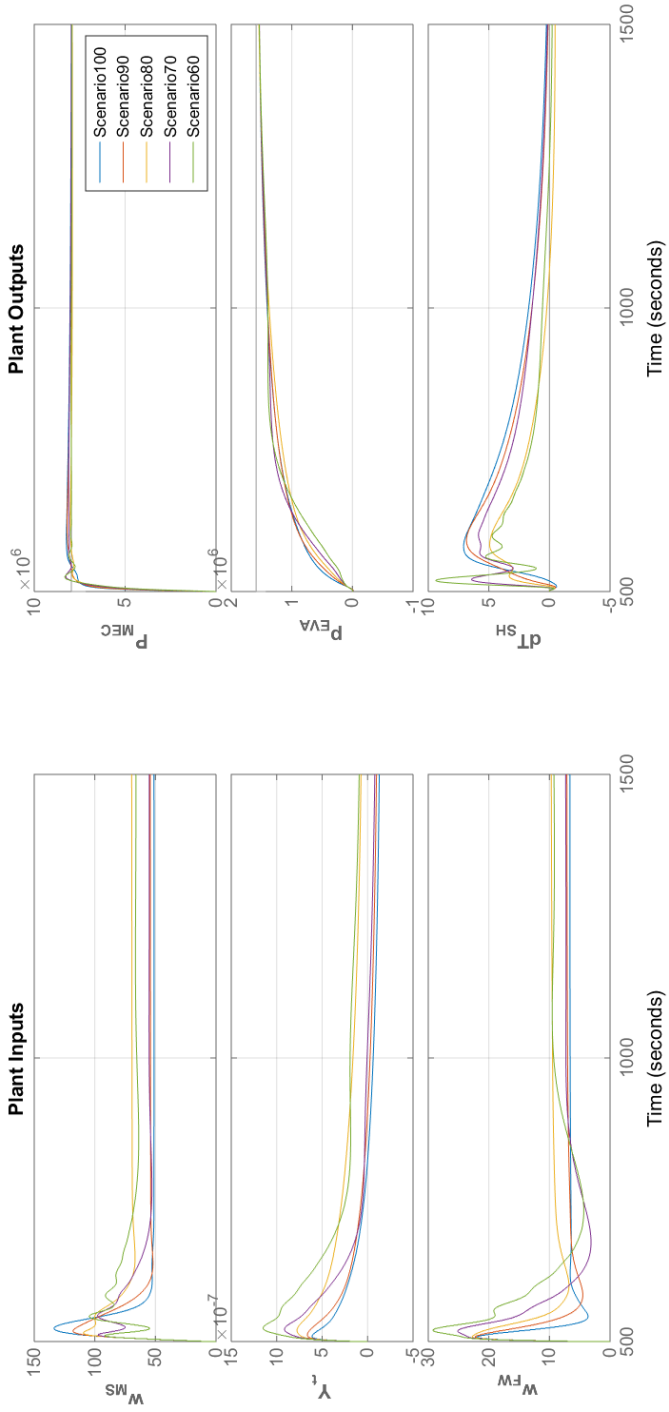

Figure 5.6: *Scenario comparison using fixed controller tuning with different linear models*

on the complete nonlinear model of the plant, allowing also to compare its results with the base control strategy. The DymolaBlock provides an interface between Dymola and Matlab.

5.2 Comparison with PID decentralized control architecture

As stated in the introduction, one of the objectives of this study is to compare the decentralized control strategy and the centralized Linear MPC control approach when the plant has to follow faster load variations. As a case of study, load ramps with a rate of 10MW/min have been tested, to evaluate the improvement that can be achieved in terms of robustness and reduced stress on the manipulated variables.

The reference signal is assumed to follow a ramp-like step, that has been made smoother at the start and at the end in order to minimize the overshoots that could arise, as discussed already for the decentralized strategy, see Chap. 4.1.1.

5.2.1 Discussion on the ramp-up:

The 60-100% ramp-up simulations are shown in Figure 5.7. Every 1000 s, a 10% increase of the load is imposed on the system as a ramp-up step of 60 s. This is translated in 10 % variation of the reference set-point of the power output (that corresponds to the load), while the reference trajectories of the other control variables are such that the plant works at the corresponding operating points. The reference set-points are plotted in Figure 5.7, dotted line. Notice that the reference set-point of the steam degree of superheating is constant (20 °C), primarily because the target on it is to make disturbance rejection. The most relevant results of the comparison for the ramp-up case are the following:

P_{mec} response: as shown in Fig. 5.7, the responses of the two control strategies are comparable since both control strategies follow well the reference signal. The main difference is that the MPC controller applies less variation than PID on the molten salt mass-flow manipulated variable (w_{MS}).
As discussed before about the adoption of the linear model at 80% load, a slight dynamic mismatch can be appreciated in the MPC ouput: while the reference signal is followed without delays at around 80%

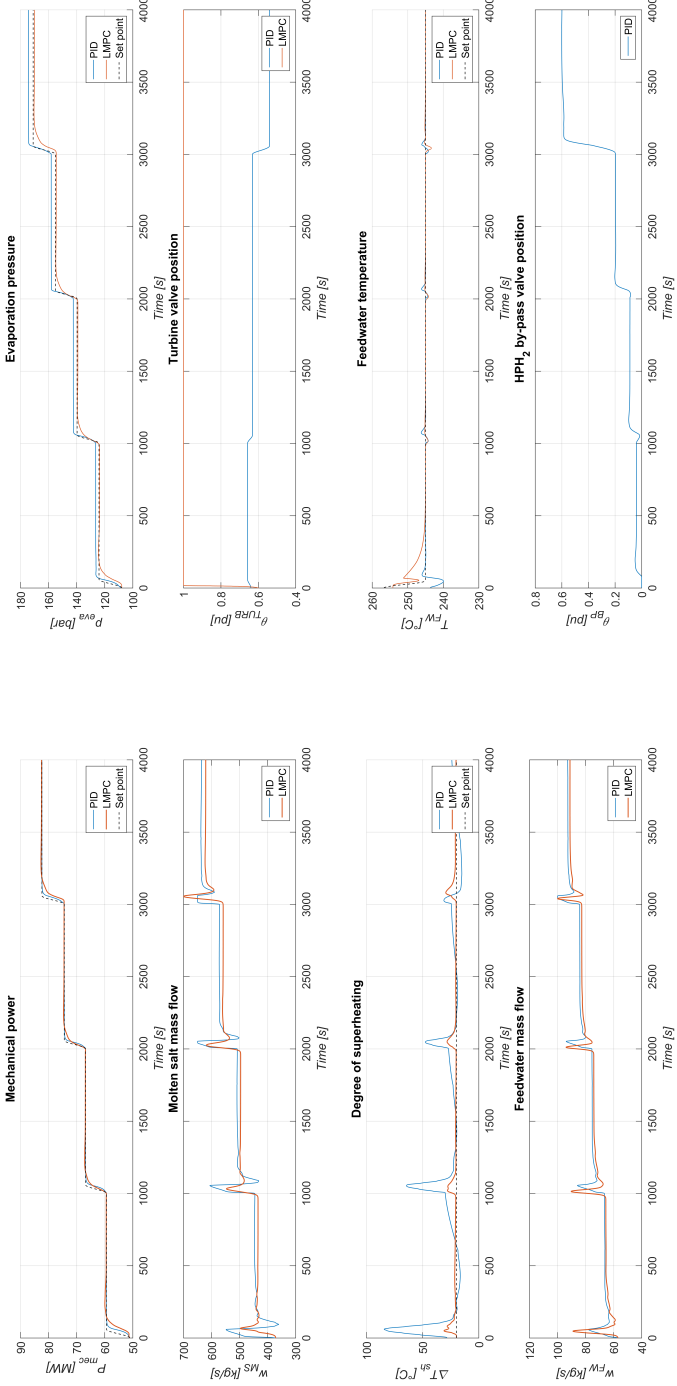

Figure 5.7: *Comparison between base control strategy and linear MPC: 60-100% ramps, 1 min each. LMPC is more robust on steam degree of superheating*

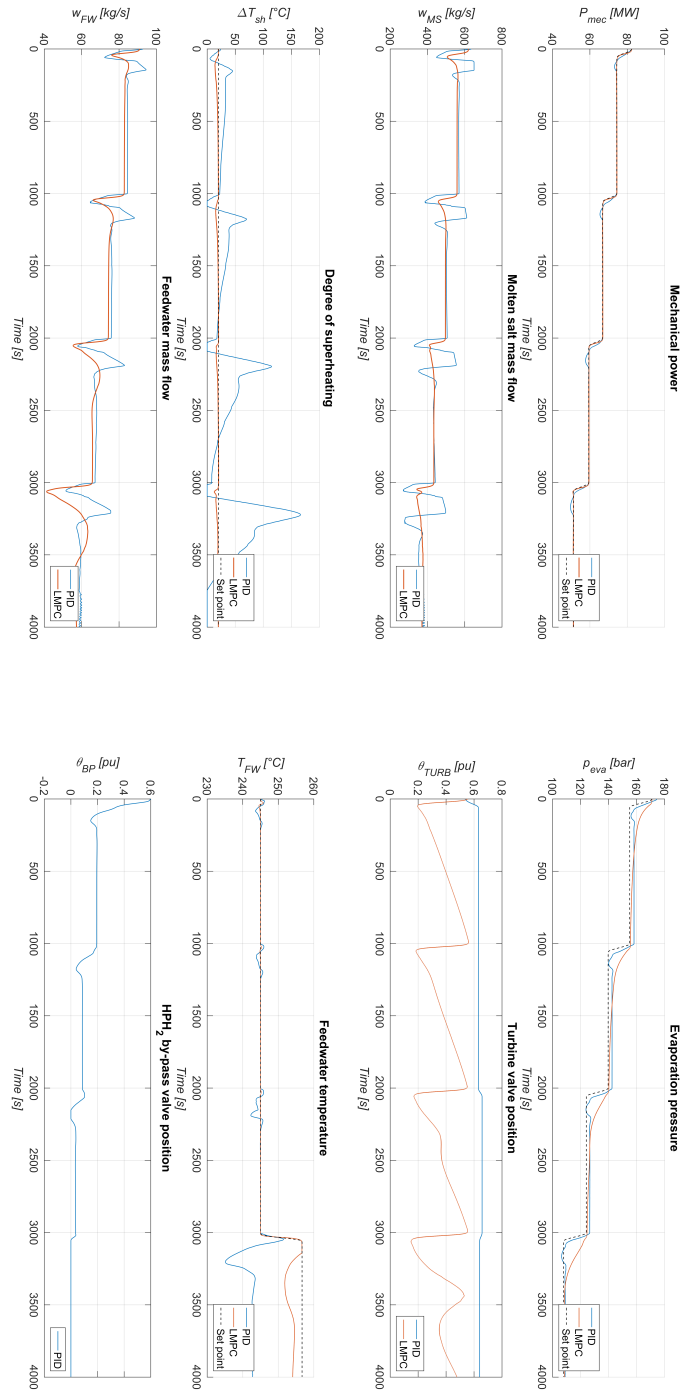

Figure 5.8: *Comparison between base control strategy and linear MPC: 100-60% ramps, 1 min each. LMPC is more robust and substantially faster in reference tracking, while acting less on manipulated variables*

of the load (as shown at top-left in Fig. 5.7), a delay is present at 60% and at 100%.

$\mathbf{p}_{eva}$ response: also in this case the responses are comparable, since both the LMPC and PID strategies do not use the valve opening manipulated variable. The interesting fact is that, if in PID the valve is kept open based on the discussion made in Chap. 3.5.3, the MPC optimizer has taken the decision autonomously, as a result of the optimization procedure.

ΔT_{sh} response: this response shows the real benefit that an advanced control strategy has over a traditional one, which does not use the model of the plant to plan the control action: in the PID control the steam degree of superheating has peaks of 70 °C (e.g. Fig. 5.7 at the bottom-left), while in the results of MPC control it never exceeds 10 °C, even near 60% when the delays in the system increase. in MPC the feedwater flow starts to act noticeably before in comparison with PID control. This is explained by the fact that the MPC control strategy is centralized and, more importantly, the predictive controller uses the model of the system to predict its future dynamic behaviour, providing a more robust control for systems with delays.

$\mathbf{T}_{FW}$ response: finally, the feedwater temperature in the MPC case presents less oscillations, even if it is controlled locally. This could be explained by the fact that, in general, there is less action on the manipulated variables, thus there is less disturbance on this loop.

5.2.2 Discussion on the ramp-down

The 100-60% ramp-down simulations are shown in Figure 5.8. In analogy with the previous case, every 1000 s, a 10% decrease of the load is imposed on the system as a ramp-down step of 60 s. This is translated in 10 % variation of the reference set-point of the power output (that corresponds to the load), while the reference trajectories of the other control variables are such that the plant works at the corresponding operating points. The reference set-points are plotted in Figure 5.8, dotted line.

In this case it is more evident that the LMPC control follows better the reference signals. The main reason of the different behavior can be noticed in the way the admittance valve is used: the LMPC acts strongly on it during the transitions, in order to permit a better tracking on power and pressure, as can be seen in the graphs (Fig. 5.8).

In MPC the degree of superheating is kept robustly at its nominal setpoint, as expected, while in the base control strategy it tends to increase in amplitude and also reaching 0 °C, which means that the separator starts the separator starts to get filled of liquid water. This is not admissible since this uncontrolled behaviour could lead to damaging the plant. Thus, the decentralized control strategy needs to be further analysed and improved, while the results given by MPC implementation are promising.

CHAPTER 6

Conclusions and future developments

In this dissertation, dynamic analysis and control of a once through steam generator for a concentrated solar power plant has been studied.
After the description of the power plant, modelled through Modelica code, the main control objectives have been identified, in terms of performance (i.e. power reference tracking) but also of security operation of the plant (i.e. avoid molten salt freezing or feedwater temperature below certain values).

The system has been linearized and studied at different operational points and, using analytical methods such as RGA matrix and Bode plots, the best couplings have been chosen, among the variables of interest. Since the plant was designed foreseeing two different configurations (as discussed in chapter 3, high load and low load), two sets of controllers have been developed, together with the definition of the switching logic. A base control strategy has been proposed, based on PI controllers, together with indices of performance and robustness (i.e. bandwidth and minimum phase margin). The presence of a non minimum phase behaviour among the transfer functions required a more in-depth study of its dynamic and a 4th order control law has been implemented in order to reach the desired performance.

The base decentralized control system has been tested on the non-linear system in realistic operational modes (i.e. dispatchability request on power signal tracking of 10MW in 15 minutes and warm start-up, from 20% to 100% load, in 10 minutes), showing its actual performances. Additionally, a faster power change rate has been tested (10MW in 1 minute) demonstrating that the system is able to fulfill the requirement, but shows a non-robust behaviour in the control of some variables such as the steam degree of superheating.

Since a more robust control action is required, the last part of the thesis deals with the implementation of linear MPC, a more advanced, centralized control strategy. The latter has proven to be more robust (i.e. action on the steam degree of superheating) in comparison with the base control strategy.

The main outcomes of the present work are:

1. thanks to the power plant model, different control logic and architectures have been tested, into an iterative process of control design and simulation which highlighted the main critical points of the process to be controlled (above all, the steam degree of superheating);

2. a decentralized control strategy has proven to be effective to satisfy the control objectives, in terms of current dispatchability and warm start-up specifications;

3. the implementation of a different, more advanced, centralized control strategy is able to highly improve the robustness and performance, when compared with the base control strategy. It also demonstrate the flexibility improvements that this plant could offer;

4. the security operation of the plant is guaranteed by both the control strategies considered. In other words, the molten salt OTSG outlet temperature is always kept above 270°C, far from its freezing temperature.

Finally, the main future developments could be:

- the enhancement of the decentralized control strategy, in order to obtain better performances, for instance the study of a dynamic decoupler between w_{MS} and w_{FW}, the introduction of dynamic filters on the feedforward action and a more in-depth study of the switching logic;

- integration of the primary frequency control within the control system;
- the optimization of some controller set-points during repetitive procedures (e.g. daily warm start-up), that could minimize a certain high level cost function, such as molten salt consumption or thermo-mechanical stresses;

Appendices

APPENDIX $\mathcal{A}$

Non-minimum Phase systems

A non-minimum phase system is a system characterized basically by an inverse response or a time delay in the open loop step response.

Consider a normalised transfer function of a system with two complex poles and one zero [10]:

$$T(s) = \frac{(s/a\zeta\omega_n) + 1}{s^2/\omega_n^2 + 2\zeta(s/\omega_n) + 1} \tag{A.1}$$

The zero is therefore located at $s = -a\zeta\omega_n$. By replacing the s/ω_n with s results in a frequency normalising effect and also a time normalising effect in the corresponding step response. Therefore the normalised version of A.1 can be rewritten as

$$T(s) = \frac{s/a\zeta + 1}{s^2 + 2\zeta s + 1} \tag{A.2}$$

The normalised transfer function can be written as the sum of two terms

$$\begin{aligned} T_n(s) &= T_1(s) + T_2(s), \\ &= \frac{1}{s^2 + 2\zeta s + 1} + \frac{1}{a\zeta}\frac{s}{s^2 + 2\zeta s + 1} \end{aligned} \tag{A.3}$$

where $T_1(s)$ can be viewed as the original term with no added zeros, and $T_2(s)$ is introduced by the zero. Since the Laplace transform of a derivative dy/dt is $sY(s)$, the step response of $T_n(s)$ can be written as

$$y_n(t) = y_1(t) + y_2(t) = y_1(t) + \frac{1}{a\zeta}\dot{y}_1(t) \tag{A.4}$$

where y_1 and y_2 are the step responses of $T_1(s)$ and $T_2(s)$ respectively. The step responses for the case when a > 0 (introduction of a left half plane zero, a = 1.1, ζ = 0.5) are plotted in Fig. A.1(a). The derivative term y_2 introduced by the zero lifts up the total response of $T_n(s)$ to produce increased overshoot. The step responses for the case when a < 0 (introduction of a right half plane zero, a = -1.1, ζ = 0.5) are plotted in Fig. A.1(b). In this case the right half plane zero, also called a non-minimum phase zero causes the response of $T_n(s)$ to produce an initial undershoot.
In general a substantial amount of literature discusses the dynamic effects of poles, but less is available on the dynamic effects of zeros.

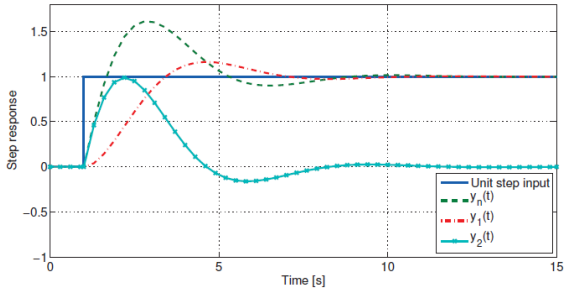

(a) Effect of a left half plane zero

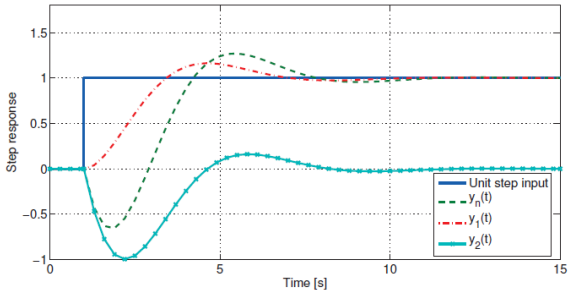

(b) Effect of a right half plane zero

Figure A.1: *Step response of $T_n(s)$*

A.0.3 A closer look at non-minimum phase zeros

In this appendix the focus is on non-minimum phase systems showing either inverse response (undershoot) or time-delays.
Undershoot refers to an initial response in the opposite direction from the steady state. According to [3] continuous systems having an odd number of real open right half plane zeros are characterised by an initial inverse response to a step input. Systems having a time-delay characteristic is a special case of non-minimum phase systems [26]. The Padé approximation is often used to approximate a time delay by a rational transfer function. Consider a first-order system with time-delay given by

$$G(s) = \frac{K}{1 + s\tau} e^{-sT} \tag{A.5}$$

K represents the gain constant, τ the time constant, and T the time-delay of the system. The Padé approximation for the term $e{-}sT$ is given by

$$e^{-sT} \cong \frac{N_r(sT)}{D_r(sT)} \tag{A.6}$$

where

$$N_r(sT) = \sum_{k=0}^{r} \frac{(2r-k)!}{k!(r-k)!}(-sT)^k \tag{A.7}$$

$$D_r(sT) = \sum_{k=0}^{r} \frac{(2r-k)!}{k!(r-k)!}(sT)^k \tag{A.8}$$

and *r* is the order of the approximation [23]. Consider the function $G(s) = 2e^{-s}/(s+1)(s+2)$. The time-delay term can be approximated by a first order Padé approximation given by

$$e^{-s} \cong \frac{2T - s}{2T + s} = \frac{2 - s}{2 + s}, \tag{A.9}$$

and therefore the rational approximated version of G(s) is given by

$$Gr(s) = \frac{(-s+2)}{(s+1)(s+2)(s+2)}. \tag{A.10}$$

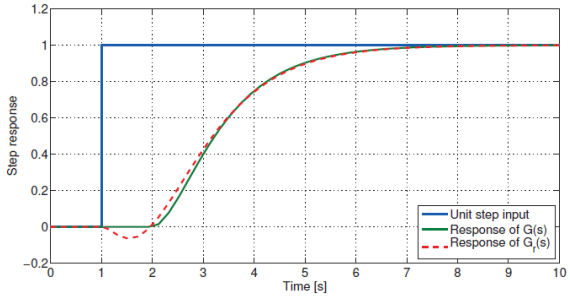

Figure A.2: *First order Padé approximation of a time-delay system*

Fig. A.2 plots the step responses of G and G_r and it is interesting to note that the response of G_r exhibits an initial inverse response. This also demonstrates a link between time delay-systems and inverse response systems.

Bibliography

[1] Impacts of intermittent renewables on electricity generation system operation. *IIT working paper*, 2012.

[2] General design specification. *Horizon 2020 Work Package 6, internal report*, 2015.

[3] Bernardo, A. & Leon de la Barra, S. On undershoot in siso systems, automatic control. *IEEE Transactions on 39(3): 578 –581*, 1994.

[4] M. Bonvini. *IndustrialControlSystems library*. Modelica. http://marcobonvini.altervista.org/ics.php?lan=ITA.

[5] F. Casella. *ThermoPower library*. Politecnico di Milano. http://thermopower.sourceforge.net/help/ThermoPower.html.

[6] E. Casati. New concepts for organic rankine cycle power systems. *PhD thesis*, 2014.

[7] E. Casati, A. Galli, P. Colonna. Thermal energy storage for solar-powered organic rankine cycle engines. *Solar Energy*, (96):205–219, 2013.

[8] ESE S.r.l. Preflexms: Making csp predictable and flexible with a once through steam generator. *http://preflexms.eu/download/csp-today-presentation/*.

[9] F. Casella, F. Donida, J. Åkesson. Object-oriented modeling and optimal control: A case study in power plant start-up. *18th IFAC World Congress (IFAC 11)*, 2011.

[10] Franklin, G. F., Powell, D. J. & Emami-Naeini, A. *Feedback Control of Dynamic Systems, 6th edn*. Prentice Hall PTR, 2010.

[11] Fthenakis V., Mason E. J.,Zweibel K. The technical, geographical, and economic feasibility for solar energy to supply the energy needs of the us. 2009.

[12] Herrmann U, Kelly B., Price H. Two-tank molten salt storage for parabolic trough solar power plants. *Energy*, (29):883–93, 2004.

[13] I. Galiana, C. Green. Let the global technology race begin. *Nature*, (462):570–571, 2009.

[14] International Energy Agency. Technology roadmap: Solar thermal electricity - 2014 edition. *www.iea.org*, 2014.

[15] Kearney D, Herrmann U, Nava P, et al. Assessment of a molten salt heat transfer fluid in a parabolic trough solar field. *J. Sol. Energy Eng*, (125):170–6, 2003.

[16] MathWorks. *Matlab Documentation*. MathWorks. http://it.mathworks.com/help/.

[17] MathWorks. *Model Predictive Control Toolbox*. MathWorks. http://it.mathworks.com/products/mpc/.

[18] Mohammed Dahleh, Munther A. Dahleh, George Verghese. *Lectures on Dynamic Systems and Control*. Massachuasetts Institute of Technology. http://tinyurl.com/jb5mvmn.

[19] PreFlexMS. Wp6: Molten salt once-through steam generator integration. *preflexms.eu*, 2015.

[20] Rian P. Vitalis. Constant and sliding-pressure options for new supercritical plants. *Riley Power Inc., a subsidiary of Babcock Power Inc.*

[21] Sathyanathan, Dr V T. Bi drum and single drum boiler compared. *www.brighthubengineering.com*.

[22] Sena-Henderson L. Advantages of using molten salts, national solar thermal test facilities. *SANDIA laboratories internal report*, 2006.

[23] Silva, G. J., Datta, A. & P., B. S. *PID controllers for time-delay systems*. Birkhauser Boston, 2005.

[24] U.S. department of energy. Linear concentrator system basics for concentrating solar power. *www.energy.gov*, 2014.

[25] Van Wyllen. *Fundamentals of thermodynamics*. John Wiley & Sons, 1994.

[26] Waller, K. V. T. & Nygardas, C. G. . On inverse response in process control. *Industrial & Engineering Chemistry Fundamentals 14(3): 221–223*, 1975.

[27] K. Weston. *Fundamentals of Steam Power*. University of Tulsa. http://www.personal.utulsa.edu/ kenneth-weston/chapter2.pdf.